NIST Technical Note 1850

Performance of Portable Radios Exposed to Elevated Temperatures

Michelle K. Donnelly
William F. Young
Dennis Camell

http://dx.doi.org/10.6028/NIST.TN.1850

National Institute of Standards and Technology
U.S. Department of Commerce

NIST Technical Note 1850

Performance of Portable Radios Exposed to Elevated Temperatures

Michelle K. Donnelly
Fire Research Division
Engineering Laboratory

William F. Young
Dennis Camell
Electromagnetics Division
Physical Measurements Laboratory

This publication is available free of charge from:
http://dx.doi.org/10.6028/NIST.TN.1850

September 2014

U.S. Department of Commerce
Penny Pritzker, Secretary

National Institute of Standards and Technology
Willie May, Acting Under Secretary of Commerce for Standards and Technology and Acting Director

Disclaimer

Certain commercial entities, equipment, instruments, standards or materials may be identified in this document in order to describe an experimental procedure, equipment, or concept adequately. Such identification is not intended to imply recommendation or endorsement by the National Institute of Standards and Technology, nor is it intended to imply that the entities, standards, materials, or equipment are necessarily the best available for the purpose.

National Institute of Standards and Technology Technical Note 1850
Natl. Inst. Stand. Technol. Tech. Note 1850, 41 pages (September 2014)
CODEN: NTNOEF

This publication is available free of charge from:
http://dx.doi.org/10.6028/NIST.TN.1850

Abstract

This study investigates the performance issues associated with the use of handheld portable radios by fire fighters working in elevated temperature environments. Radios may be vulnerable to elevated temperatures that can be encountered during firefighting activities. Controlled, repeatable, well characterized test methods were used to measure radio performance. The radios were exposed to elevated temperature environments for specific temperatures and times. At Thermal Class I conditions of 100 °C for 25 min, all of the radios tested maintained frequency stability. At Thermal Class II conditions of 160 °C for 15 min, all of the radios tested experienced signal drift of the mean maximum-power frequency. Some of the radios stopped transmitting during the testing.

Table of Contents

Introduction

Portable handheld radios are widely used during firefighting operations, and these radios are often exposed to the elevated temperatures that are typically present in a fire environment. Radios, like other electronic equipment, can be vulnerable to elevated temperatures. Previous investigations have shown that radios may suffer physical damage, such as melting and deforming, as well as operational difficulties when exposed to elevated temperature environments [1]. Performance problems with portable radios have been identified by the National Institute for Occupational Safety and Health (NIOSH) as contributing factors in some fire fighter fatalities [2]. To investigate the impact of elevated temperatures on radio operations, experiments were conducted to measure the performance of portable radios exposed to elevated temperatures. The goal of this investigation is to develop scientifically based performance standards for fire fighter portable radios.

Currently, the National Fire Protection Association (NFPA) has no specific standards in place for portable radios and other two-way communication devices. These types of devices are broadly covered by NFPA 1221: Standard for Installation, Maintenance and Use of Emergency Services Communications Systems [3]. The general usage of two-way portable equipment is referred to in NFPA 1221 Section 9.3.6. The only requirements in this standard relating to radio operation in the fire environment are found in Section 9.3.6.2, which states "Portable radios shall be manufactured for the environment in which they are to be used and shall be of a size and construction that allow their operation with the use of one hand," and Section 9.3.6.12, which states "Portable radios used by first responders who might encounter hazardous conditions likely to cause fire or explosion because of the release of flammable liquids or gases shall be rated as Intrinsically Safe by a recognized testing authority, if determined necessary by the AHJ." No further information is given to specify details of the "environment" in which the radios are to be used, and no testing procedures or performance criteria are outlined in the standard.

To address the lack of performance standards for fire fighter portable radio equipment, the NFPA Technical Committee for Electronic Safety Equipment has proposed the development of a standard for portable radios used by emergency service personnel. The information in this paper provides data and performance measurements relevant to the development of the new standard.

Because of the lack of standards for portable radios, operation guidelines and performance criteria have been left to the radio manufacturers. Many of the manufacturers list maximum operating temperatures of 60 °C for the radios to be used by fire fighters. This temperature falls well below temperatures that a fire fighter could encounter while operating in a fire environment. Previous work studying the performance of electronic equipment used by first responders in elevated temperature environments led to the development of a Thermal Class system for categorizing the operation of electronic equipment exposed to thermal conditions [4].

Table 1 shows the designated air temperature and time duration for the four Thermal Classes. These Thermal Classes were used to guide this investigation on radio performance at elevated temperatures. The Thermal Classes were developed with the specific goal of providing testing conditions for fire fighter equipment, and do not attempt to classify the fire fighting environment itself.

The research discussed in this paper focuses on the performance of portable radios exposed to Thermal Class I and Thermal Class II conditions. Thermal Class I conditions represent temperatures that the equipment may be exposed to when a fire fighter is fighting a small fire in a room, or when fighting fires from a distance [5, 6]. Thermal Class II conditions represent temperatures the equipment may experience during more involved fire fighting operations, such as when fighting a totally involved fire, or when outside a room that experiences flashover conditions [7, 8]. These experiments did not expose the radios to conditions of Thermal Class III or beyond.

Table 1. Thermal Classes for Electronic Equipment Exposure

Thermal Class	Time Duration	Temperature
Class I	25 min	100 °C (212 °F)
Class II	15 min	160 °C (320 °F)
Class III	5 min	260 °C (500 °F)
Class IV	< 1 min	> 260 °C (>500 °F)

This publication is available free of charge from http://dx.doi.org/10.6028/NIST.TN.1850

Apparatus and Equipment

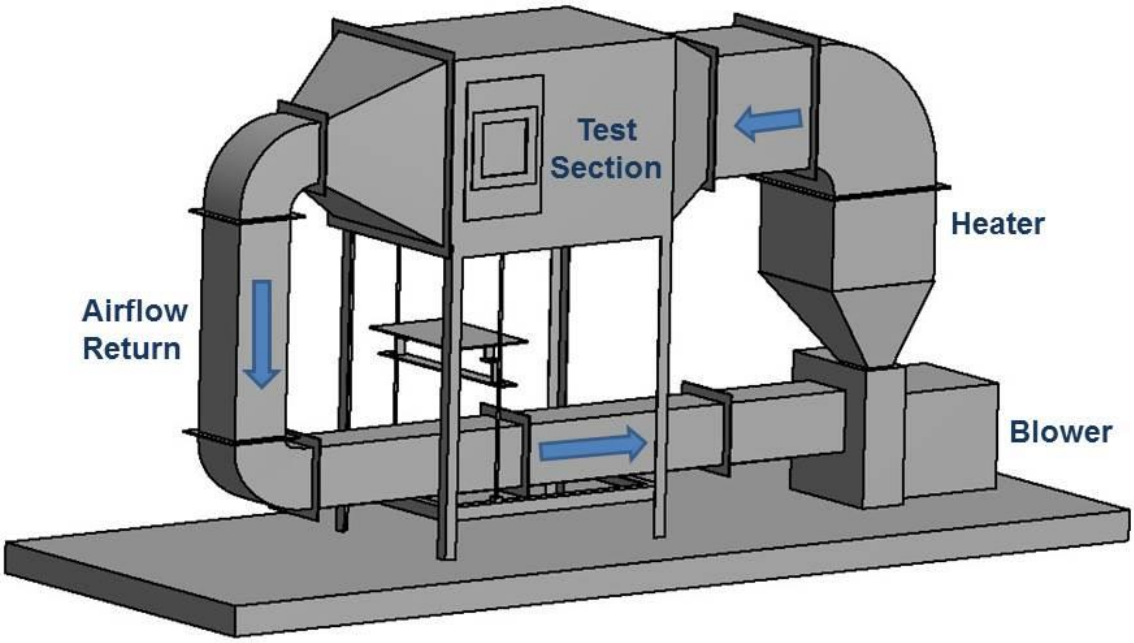

Figure 1. NIST Thermal Exposure Flow Loop

The NIST thermal exposure flow loop provided the elevated temperature environment for the portable radio exposure experiments. The thermal exposure flow loop is electronically controlled with recirculating airflow, providing a well-defined, repeatable, convective heating environment. The flow loop can be used to expose items to elevated temperatures with varying airflow rates and thermal conditions. Figure 1 is a diagram of the thermal exposure flow loop apparatus. The main parts of the flow loop are the blower, heater, test section, and airflow return. The flow loop measures 4.09 m in total length from the heater section to the airflow duct, not including the blower. The top of the flow loop is at a height of 2.49 m. The maximum width of the flow loop (0.91 m) occurs at the test section. A more detailed diagram of the flow loop is included in the Appendix, Figure A1.

This publication is available free of charge from http://dx.doi.org/10.6028/NIST.TN.1850

The thermal exposure flow loop provides an environment for exposing items to a convective heat flow at a controlled air temperature up to 300 °C. The air is heated to the desired temperature using a 50 kW electric air duct heater. A variable speed electric blower located below the heater circulates the air through the flow loop. The flow can be adjusted, allowing for control of the air velocity at the test section from 0.5 m/s to 1.4 m/s. A return airflow duct carries the air back to the blower, where it is recirculated through the loop.

Items to be tested are mounted to a 0.60 m by 0.38 m moving platform located directly below the test section, which is used to insert and remove items from the test section. The radio was secured on the platform in the upright position by a support post and equipment holder. A photograph showing one of the radios on the platform is shown in Figure 2. The support post and holder are adjusted so the center of the radio body is located at the center of the cross sectional area of the test section when the radio is inserted in the flow loop. The grips of the holder in contact with the radio are covered with sleeves made from aramid fabric to insulate the grips and reduce heat transfer from the grips to the radio. Insulated wiring was used to further secure the radio in place.

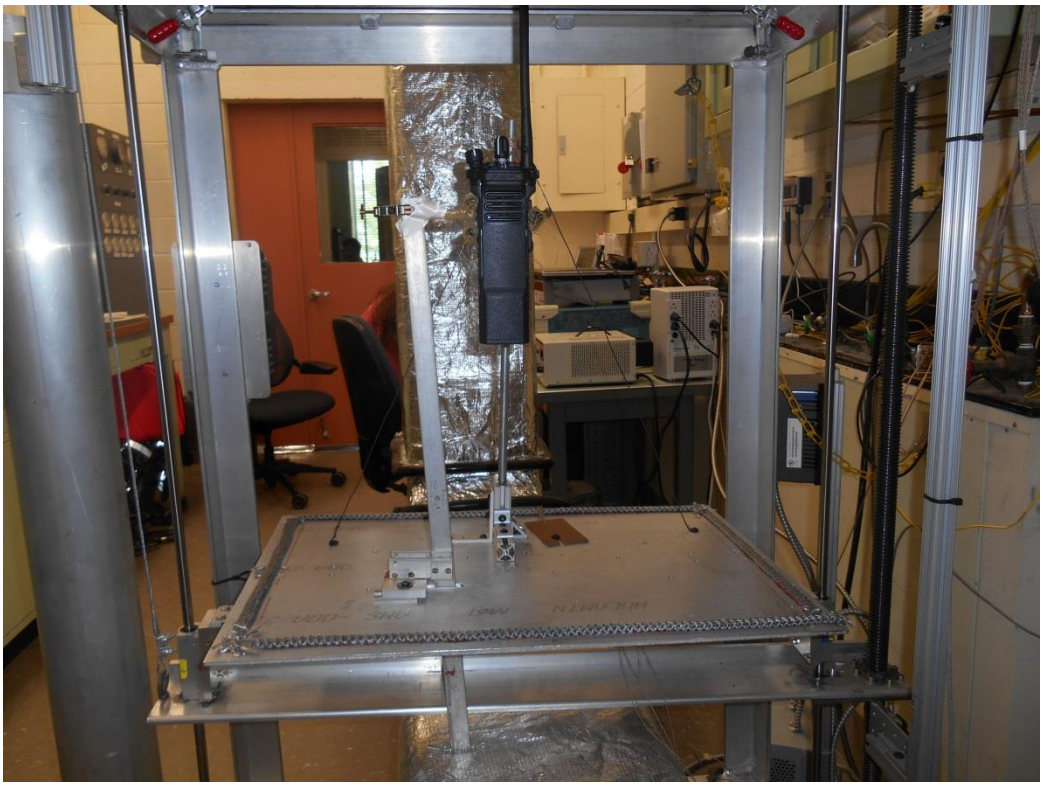

Figure 2. **Photo of radio mounted on the flow loop platform**

The test section of the flow loop has a 0.91 m by 0.91 m cross sectional area and is 1.3 m in length. Instrumentation inside the flow loop measures airflow velocities and temperatures. Experiments may be performed at a constant temperature and velocity or these may be varied during testing. A diagram showing the side view of the test section of the flow loop, with detailed dimensions and instrumentation locations is shown in the Appendix, Figure A2. The bottom of the test section is equipped with a sliding door. The door opens to allow items on the platform below to access the test section. When the platform is fully raised, it seals the bottom opening of the test section.

The airflow velocity in the test section was measured using three bidirectional velocity probes. The center velocity probe was placed at the center of the cross sectional area of the flow loop, 0.6 m upstream of the radio test location, as shown in Figure A2. An upper velocity probe was located 23 cm directly above the center probe and a lower probe was located 23 cm directly below the center probe. All three probes were positioned to measure the velocity in the direction of the airflow. To obtain velocity measurements, the probes used pressure transducers that measured the differential pressures, and thermocouples that measured the temperatures at the probe locations. The pressure transducers were factory calibrated, with an accuracy of ± 1% [9], and the experimental uncertainty was estimated to be ± 10 %. The uncertainty of the thermocouple measurements was ± 15 %, as discussed below. For all of these tests, the blower was set to the maximum rate, resulting in an average airflow velocity in the test section of 1.4 m/s. The estimated total expanded uncertainty (two standard deviations) for the velocity measurements was ± 18 %.

Temperatures were measured using type-K thermocouples. The sampling rate for the thermocouple measurements was 1 Hz. Thermocouples located inside the flow loop measured the airflow temperature at various locations, as shown in Figure A2. Stainless steel sheathed thermocouples, 3.2 mm diameter, were located next to each of the bidirectional velocity probes to measure the local temperatures. Ten bare-bead thermocouples, nominally 1 mm diameter, were positioned on a vertical mount located 0.4 m upstream of the test location and centered 0.46 m from each of the vertical walls of the test section. The thermocouples were spaced 7.6 cm apart along the vertical mount, starting 7.6 cm below the ceiling of the test section.

The thermocouples were subject to measurement uncertainty due to material variation and radiative heating from the flow loop. The measurement uncertainty (one standard deviation) for the thermocouple wire was ± 2.2 °C as listed by the manufacturer [10]. The estimated experimental uncertainty (two standard deviations) for the thermocouple measurements was ± 15 %. The uncertainties in the remainder of the paper are expressed in terms of estimated experimental uncertainty (two standard deviations).

Elevated temperature exposure tests were conducted at two of the Thermal Class conditions described in Table 1, namely Thermal Class I conditions at nominally 100 °C for

25 min and Thermal Class II conditions at nominally 160 °C for 15 min. The temperature in the test section of the flow loop was measured using the bare-bead thermocouple located on the vertical mount at the center of the cross sectional area of the test section, which corresponded to the height and depth of the center of the radio body during testing. This thermocouple was used to control the flow loop heater setting. An example of the temperatures measured in the test section of the flow loop during one of the Thermal Class I exposure tests nominally at 100 °C is shown in Appendix Figure A3. The plot shows the temperature measured by the thermocouple located on the vertical mount at the centerline, as well as the temperatures measured by the thermocouples 7.6 cm above and 7.6 cm below the centerline. Temperatures at these heights are shown because they fall within the height locations of the radio during testing. The average temperature at the centerline was 100.2 °C ± 1.7 °C. The average temperature 7.6 cm above the centerline was 100.2 °C ± 1.4 °C, and the average temperature 7.6 cm below the centerline was 100.1 °C ± 1.7 °C. Similar measurements were made for each test, resulting in average temperatures between 100 °C and 103 °C, with a maximum expanded variance of 3.2 °C.

For the Thermal Class II exposure tests nominally at 160 °C, an example of the temperatures measured in the test section is shown in Appendix Figure A4. Again, the temperatures measured by the thermocouples located on the vertical mount at the centerline, 7.6 cm above and 7.6 cm below the centerline are plotted. For the test shown, the average temperature at the centerline was 160.1 °C ± 1.7 °C. The average temperature 7.6 cm above the centerline was 160.4 °C ± 1.2 °C, and the average temperature 7.6 cm below the centerline was 159.8 °C ± 1.7 °C. Similar measurements were obtained for each of the experiments at Thermal Class II conditions with average temperatures measuring between 159 °C and 162 °C with a maximum expanded variance of 2.7 °C.

This publication is available free of charge from http://dx.doi.org/10.6028/NIST.TN.1850

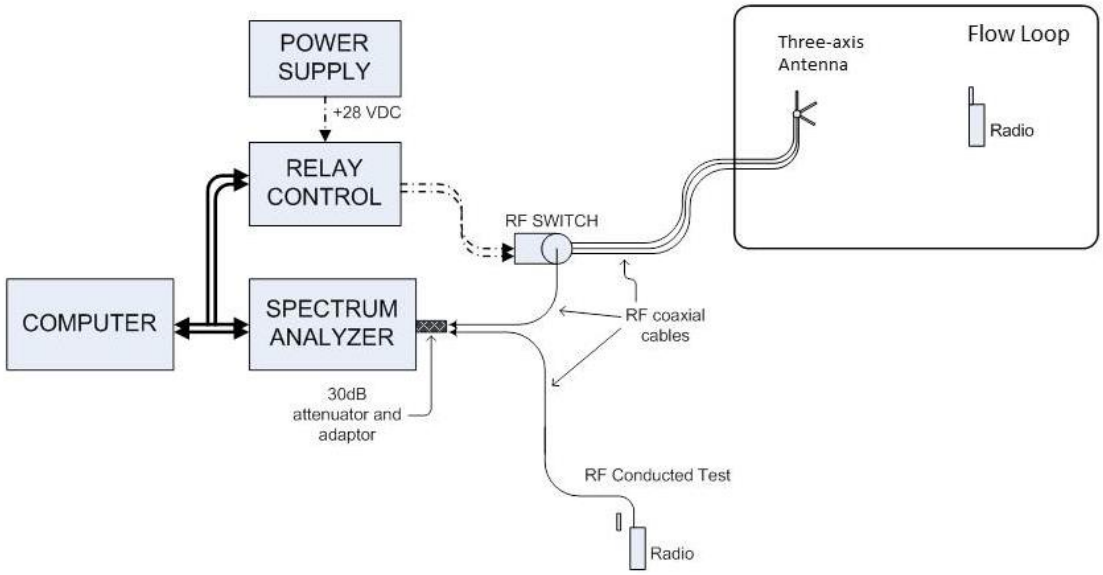

Figure 3. **Diagram of Radio Frequency Sampling System**

To characterize the radio performance during the elevated temperature testing, a radio frequency (RF) sampling system was developed to measure the RF signal levels from a transmitting radio. A diagram of the RF sampling system is shown in Figure 3. To measure the radio signal while the radio was transmitting using its antenna, a three-axis receiving antenna was located in the flow loop and connected through an RF switch to a spectrum analyzer. Each of the three-axis antenna elements was orientated on a different axis of polarization, although the relative orientations were not perfectly orthogonal. A relay control was used to send +28 VDC to the RF switch. The RF switch systematically cycled through each port of the three-axis receiving antenna, and the resulting RF signals were sent to the spectrum analyzer. A 30 dB attenuation pad was placed on the spectrum analyzer to provide overload protection. Prior to testing, appropriate spectrum analyzer settings for comprehensive frequency coverage and optimal sampling rate were determined. During the test process, a computer was used to supply the spectrum analyzer settings, calibrate the spectrum analyzer, set the RF switch through the relay control, read the spectrum analyzer, and collect and save the data. Antenna settings, data selection and collection timing were also controlled via the computer.

The RF sampling system was also used to measure the signal directly from the radio into the spectrum analyzer, here referred to as RF conducted tests. The RF conducted tests were performed to obtain baseline RF measurements, as explained in the Testing Procedure section

below. For the RF conducted tests, the three-axis antenna and RF switch were bypassed and the radio was connected directly to the spectrum analyzer through a coaxial cable.

Testing Procedure

Prior to each elevated temperature test, an RF conducted test was performed for each radio to establish a baseline signal for the radio. For the RF conducted tests, the radio was located outside the flow loop and was at ambient temperature. The radio antenna was removed and a coaxial cable was connected from the radio directly to the spectrum analyzer. The signal was triggered by pushing the push-to-talk (PTT) button on the radio. The RF signal was measured for 60 s. The radio antenna was then replaced, and the portable radio was readied for elevated temperature testing.

For each elevated temperature test, the portable radio was secured in the equipment holder on the platform below the test section of the flow loop. The RF sampling system was used to collect an initial RF signal as measured by the three-axis antenna at ambient temperature. As with the RF conducted test, the radio signal was triggered with the PTT button, and 60 s of signal data was collected. But unlike the RF conducted test, the signal was transmitted via the radio antenna, received by the three-axis antenna, and relayed to the spectrum analyzer through the RF switch system.

Next, the flow loop blower and heater were started. The airflow velocity and temperature were selected. When the required airflow velocity and temperature were reached, the bottom of the flow loop test section was opened and the equipment platform was raised into the test section. The platform was fully raised, exposing the radio to the heated airflow, and closing the bottom of the test section. At periodic intervals throughout the experiment, the PTT button on the radio was depressed using a remote activating arm, and the resulting RF signal was collected by the three-axis antenna and measured using the RF sampling system. After a predetermined time, the platform with the radio equipment was removed from the flow loop. Outside of the flow loop, within 60 s to 90 s after removal of the radio from the flow loop, a final measurement of the RF signal was collected using the RF sampling system in the three-axis antenna configuration.

Five different radio models were tested. Three model A radios were tested, and one each of models B, C, D, and E were tested at each Thermal Class condition. In these tests, the radio was positioned so that the front face of the radio faced into the direction of the flow. In addition, the radio was always fully exposed to the flow. It was not placed in any pocket or other protective device as in previous tests [1]. The purpose for this testing was to provide information for development of a standard, so the worst case scenario of a fully exposed radio was chosen.

All experiments were performed with the radios set to transmit at a frequency of 162.175 MHz in the very high frequency (VHF) band. This was a local government frequency

that was available to use for testing. Because the housing materials, oscillator circuity, other radio components are common to all radios, similar results are expected for radios operating in other frequency bands.

Battery Considerations

The batteries used to operate the radios under elevated temperature conditions are a concern due to the adverse effects of heat on batteries. It is important for the batteries to be able to operate safely when exposed to elevated temperatures. Recently, manufactures have been using new battery technologies to decrease the size and weight of the batteries and to increase performance. Most radio manufacturer specifications list the maximum operating temperature for the batteries as 60 °C.

Some batteries may be hazardous when used in an elevated temperature environment. Lithium-ion (Li-ion) batteries may pose a danger of fire or explosion when operated in an elevated temperature environment. Exposure to elevated temperatures can cause a decomposition reaction in the Li-ion batteries, which can eventually lead to thermal runaway [11, 12]. During thermal runaway, the temperature and pressure inside the battery rises faster than can be dissipated, which can result in fire or explosion. The critical temperature for thermal runaway depends on the specific chemical makeup, but can occur at temperatures around 150 °C to 175 °C [12, 13]. As battery technologies are evolving, battery manufacturers are developing approaches to improve the thermal performance of these batteries and to safeguard against thermal failures by installing shutdown separators [13] or adding thermal runaway inhibitors [14].

Batteries for portable radios are not standardized. Most batteries are specific to the manufacturer and even to the model of radio. Some radios on the market today offer options for batteries of different chemical make-up. In some cases, third party batteries are also available. In most cases, the battery housing makes up some of the body of the radio itself. Because batteries contribute to the structural integrity of the radio, impact radio performance, and may introduce additional hazards, it is crucial that the specific battery type used in the radio during fire fighting operations is included in any elevated temperature exposure testing related to standards certification. Any fire fighter radio standard should require that the radio body and battery be tested together as a unit, and that standard certification applies to the radio and battery as a unit.

For some of the radios tested in this set of experiments, multiple battery types were available. All of the testing described in this document was performed using radios powered by nickel-metal hydride (Ni-MH) batteries. The batteries were supplied by the radio manufacturers. Third-party batteries were not used for these tests.

This publication is available free of charge from http://dx.doi.org/10.6028/NIST.TN.1850

Results and Discussion

Conducted Results

The data collected during the measurement process are presented in several forms. The RF signal as measured directly by the spectrum analyzer was a measurement of the signal power over the frequency spectrum. When the radio was placed in transmit mode, an RF signal was generated with the peak signal power ideally occurring at the radio transmitter frequency. Figure 4 shows a sample RF signal for a conducted test as measured by the spectrum analyzer. In this sample signal, the signal power was concentrated at the radio's selected transmission frequency of 162.175 MHz. The plot represents a snapshot of the RF signal at a given time. Radio power is shown in decibel-milliwatts (dBm), which is a typical format used in the communication industry. Power in dBm is plotted on a logarithmic scale, and is offset such that 0 dBm represents 1 mW. A larger number corresponds to a higher power reading. See Appendix B for further explanation of the radio power measurements. For all of the signal measurements by the spectrum analyzer, a 30 dB attenuation pad was used to protect the equipment from overload.

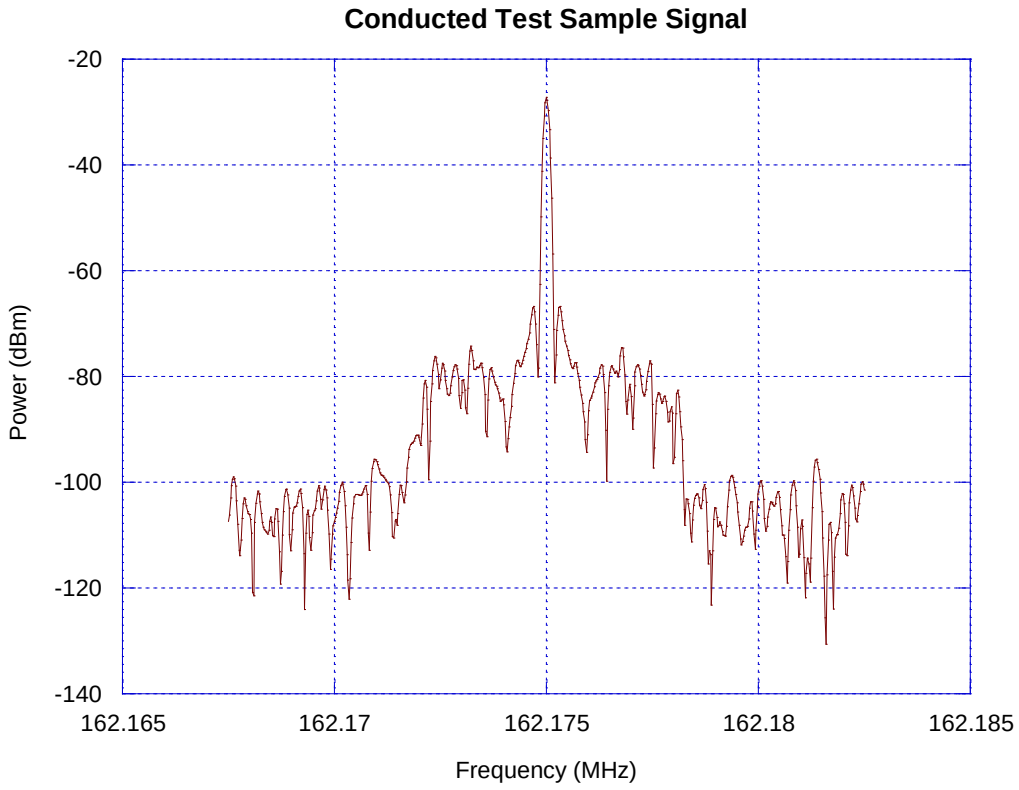

Figure 4. RF measurement for a conducted test as displayed on a spectrum analyzer

The power level as a function of frequency and time, or power spectrogram, shows the transmitted power across the frequency band. On the spectrogram, the x-axis represents time, the y-axis represents frequency, and the color value represents the power level. Figure 5 shows the spectrogram for the RF-conducted tests. The RF-conducted test duration was just over 60 s and the frequency band was approximately 15 kHz centered on the nominal transmitter frequency of 162.175 MHz. Only the carrier frequency was of interest; capturing the full 25 kHz channel was not necessary. Since the radios were operating at room temperature during these tests, the maximum-power frequency tracked 162.175 MHz quite well, as expected. This frequency of the maximum-power corresponds to the carrier frequency and only varied in the case of radio A1. The other six radios did not demonstrate any variation in the frequency of maximum transmitted power. The results are plotted in Figure 6, which shows the mean maximum-power frequency.

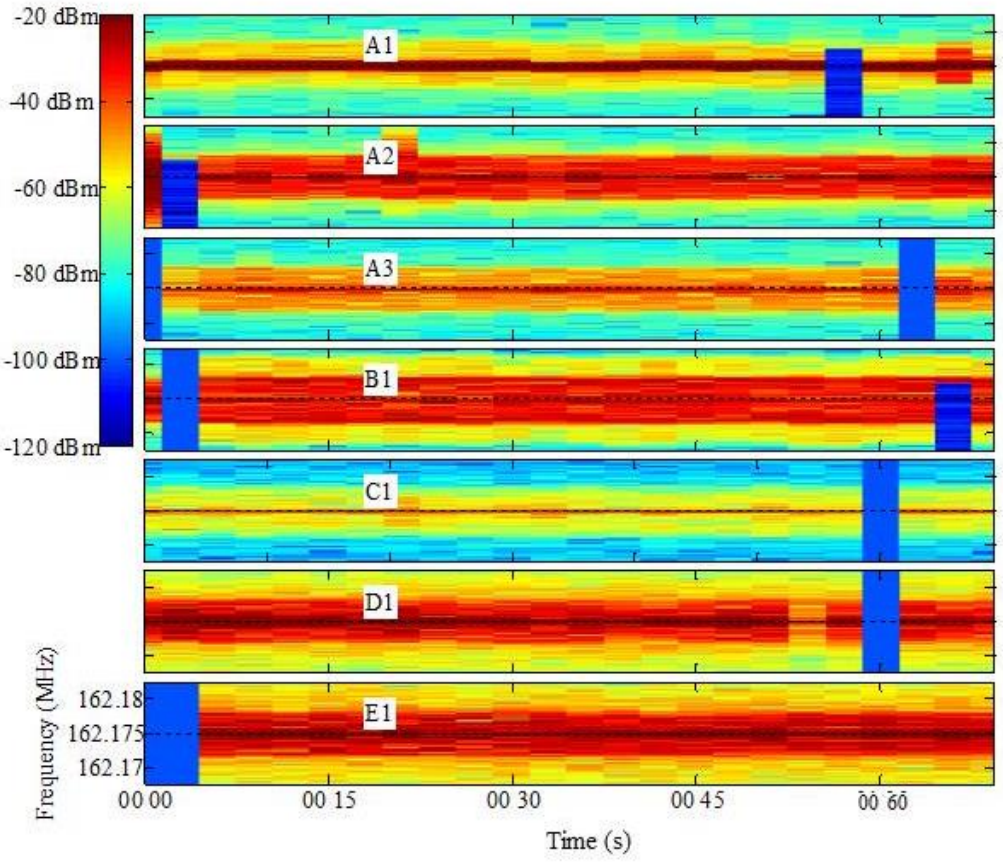

Figure 5. Conducted power versus frequency and time measurement results for the seven radios. The letter labels correspond to the radio, e.g., A1 is radio A1. The solid blue values represent time when transmission data were not collected. The frequency range shown is identical for all seven tests.

This publication is available free of charge from http://dx.doi.org/10.6028/NIST.TN.1850

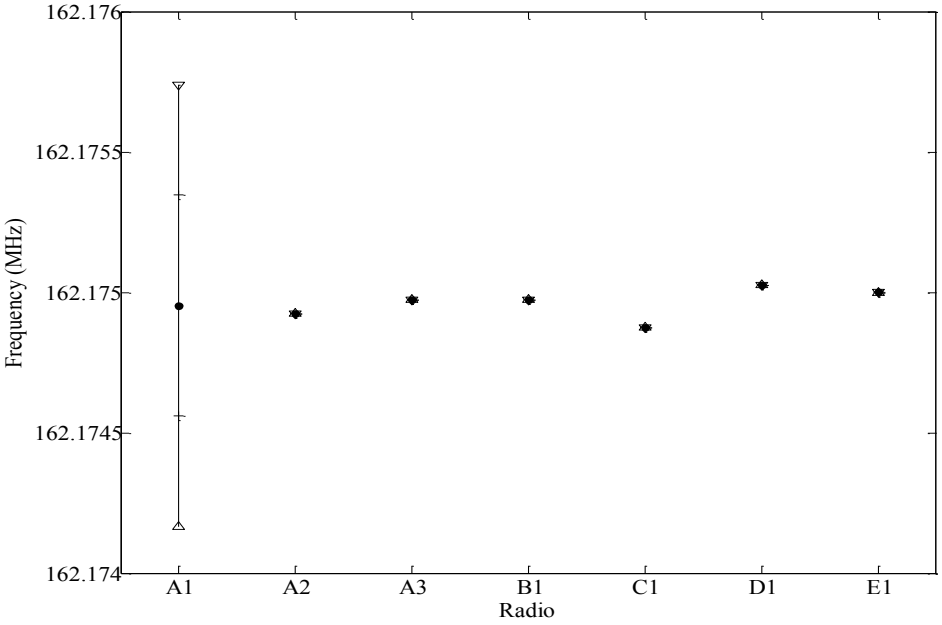

Figure 6. Mean maximum-power frequency for the RF conducted tests. The maximum power frequency corresponded to the carrier frequency. Dash marks indicate 1σ, and triangles indicate 2σ. The standard deviations, 1σ and 2σ, in the maximum-power frequency for radio A1 were large relative to the standard deviations measured for the other radios. For radios A2, A3, B1, C1, D1 and E1, 1σ and 2σ were small and are barely visible behind the data symbols in the plot.

To relate the data to a common radio performance metric, Figure 7 shows the maximum-power frequency as a deviation from the nominal carrier frequency of 162.175 MHz. In addition, these resulting frequency deviations are expressed in parts-per-million (ppm), and provide a common measure of frequency stability (see Figure 7). The Federal Communications Commission (FCC) and the radio manufacturers specify acceptable frequency drift limits in units of ppm. In order for the received signal to be properly demodulated and to avoid interfering with adjacent radio frequency channels, the transmitted signal must remain very near the assigned frequency. Since the amount of acceptable drift in frequency is quite small relative to the carrier frequency, the change in frequency is measured in ppm rather than percent. The equation for computing the change in frequency relative to the nominal carrier frequency is as follows:

$$\text{Frequency drift}\,(\text{ppm}) = 1\,000\,000 \times \frac{\Delta f}{f_c}\ , \qquad (1)$$

where f_c is the carrier frequency and Δf is the difference between the measured carrier frequency and the nominal carrier frequency.

As Figure 7 shows, only radio A1 demonstrated any significant variation in frequency stability. The other six radios exhibited a frequency deviation of less than 1 ppm, with 2σ much less than 1 ppm for all the measurements. Radio A1 showed a mean frequency deviation of less than 1 ppm, but 2σ was slightly greater than 5 ppm for that frequency deviation. These data can be compared with standards such as the Telecommunications Industry Association (TIA) on land mobile radios [15], where the performance criteria are derived from the FCC regulations 47 CFR 90.213 and 90.539. Table 30 of TIA-603-D states that the frequency stability shall be within 5.0 ppm for the 162.175 MHz radios. The RF conducted test results show that while at ambient temperature before the elevated temperature exposure tests, the radios were all operating within the FCC frequency stability limits and the TIA standard.

Note that the term deviation is used in two contexts here; one with respect to the change in frequency relative to the carrier frequency and the other, σ, as in the statistical standard deviation of the measurement. The uses are consistent with the standard language for describing the two measures.

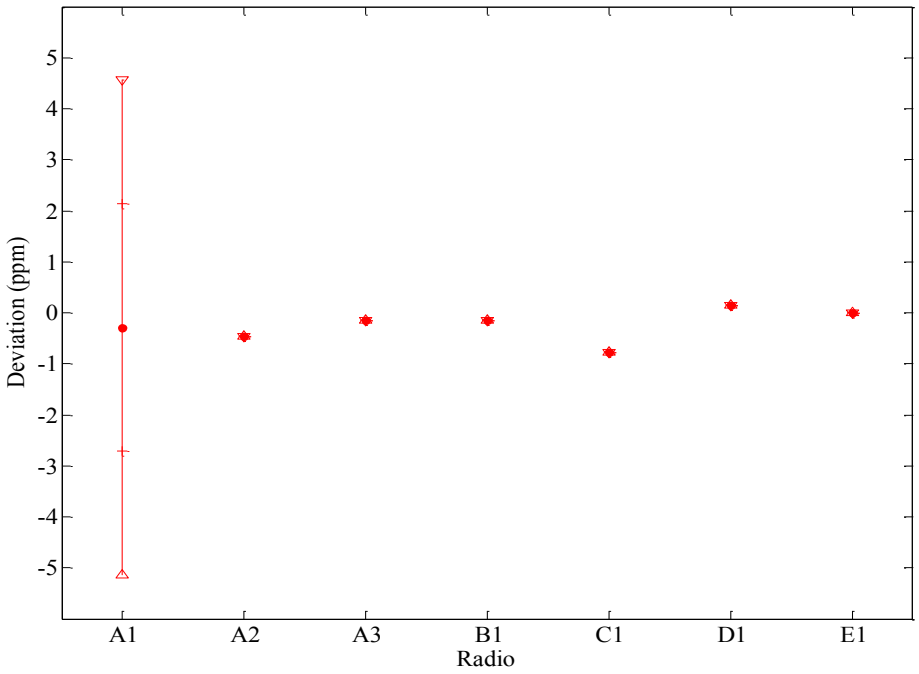

Figure 7. Mean maximum-power frequency deviation for the RF conducted tests. The frequency deviation was relative to 162.175 MHz. Dash marks indicate 1σ, and triangles indicate 2σ. For all radios except A1, 1σ and 2σ were small, and are barely visible behind the data symbols. For radio A1, 1σ was within the TIA-603-D standard range, however 2σ fell slightly out of the ± 5 ppm range. For the other radios, 1σ and 2σ were well within the ± 5 ppm set forth in the TIA-603-D standard [10].

100 °C Results

The first set of experiments at elevated temperature conditions were performed at Thermal Class I conditions of 100 °C for 25 min. In these tests, the three-axis antenna was located inside the flow loop and the radio used the manufacturer supplied antenna. Due to objects in the laboratory, the metallic walls of the heat flow loop, the relatively close proximity of the antenna probe to the transmitting radio, and other experiment limitations, accurate transmitted power levels were not measurable. However, the carrier frequency was identified by the maximum-power frequency. Results are shown for each of the three antenna elements.

Figure 8 shows the spectrograms for antenna 1. The carrier frequency is identified by its relatively high power centered near 162.175 MHz. The solid blue sections (i.e., -100 dBm) indicate times when the radio was not transmitting. White sections of the plot indicate that the test was completed. When the radio was transmitting, the measured power level varied across the frequency range with a maximum level near 162.175 MHz. The radios were on for at least 60 s. After 60 s, some of the radios were turned on again; this event is evident by a narrow blue solid line in an otherwise active transmission time. Radio B1 also showed a very narrow active region when the radio was inadvertently on. The data from this short transmission were not used in the subsequent analysis. Figure 9 and Figure 10 show the results for the other two antenna elements. The power levels are different, but the same behavior in the carrier frequency was observed.

An important consideration when interpreting the frequency variation is that the data were collected in a confined metallic structure with the three-axis receiving antenna located in the near-field (electromagnetic field) of the transmitting radio. This can cause more variability in the maximum-power frequency than if an RF conducted measurement process is used. The drawback of an RF conducted measurement is that the radio antenna is not included. Thus, to test the radios as complete units, these tests were performed with the radio antenna transmitting to the receiving antenna. The key performance indicator here is the stability of the mean maximum-power frequency over time.

This publication is available free of charge from http://dx.doi.org/10.6028/NIST.TN.1850

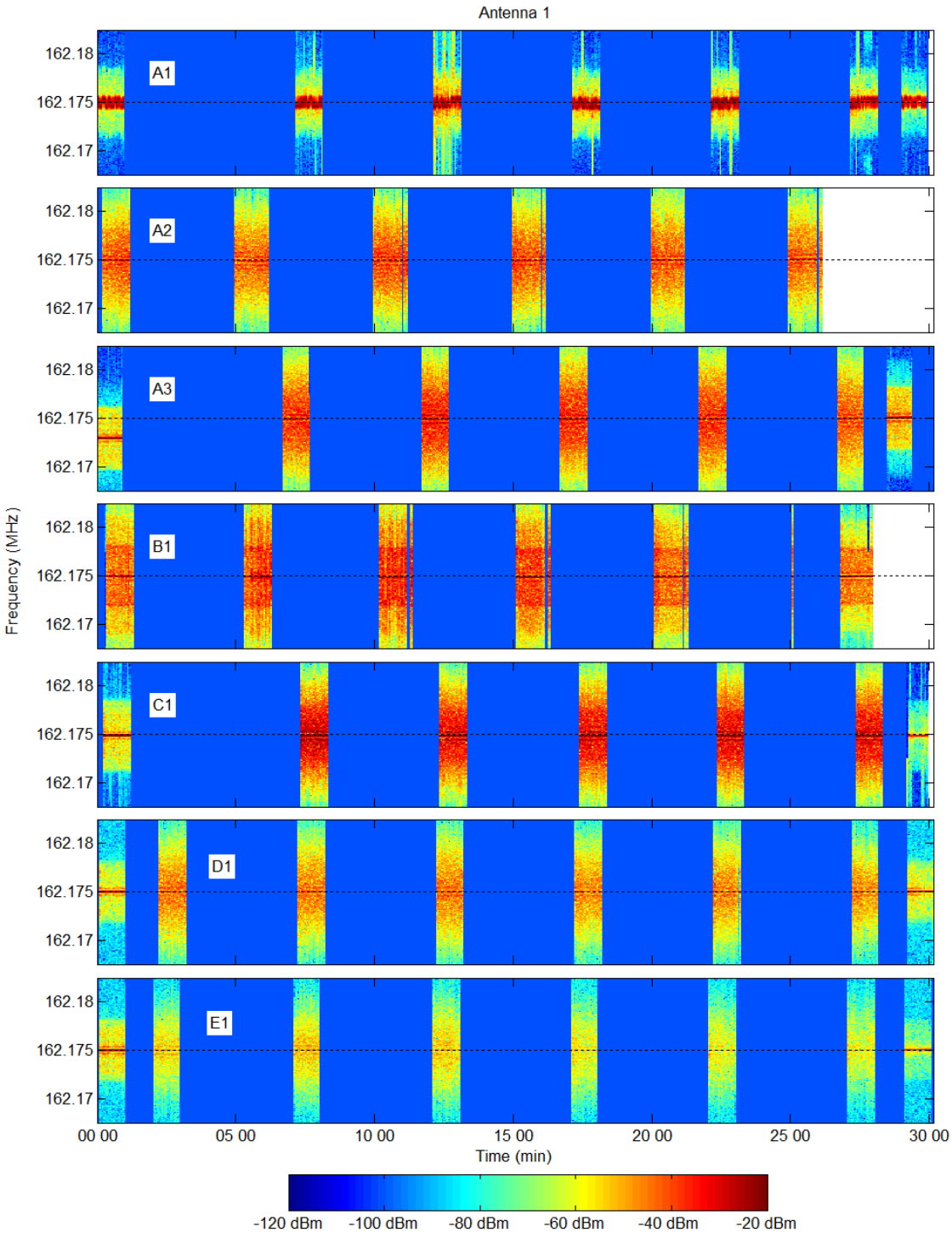

Figure 8. Power versus frequency and time measurement results for Antenna 1 at 100 °C for 25 min. The letter labels correspond to the radio. The blue sections of the plots indicate the radio was not transmitting and the white sections indicate that the test was completed. The dotted center line represents the nominal frequency of 162.175 MHz.

This publication is available free of charge from http://dx.doi.org/10.6028/NIST.TN.1850

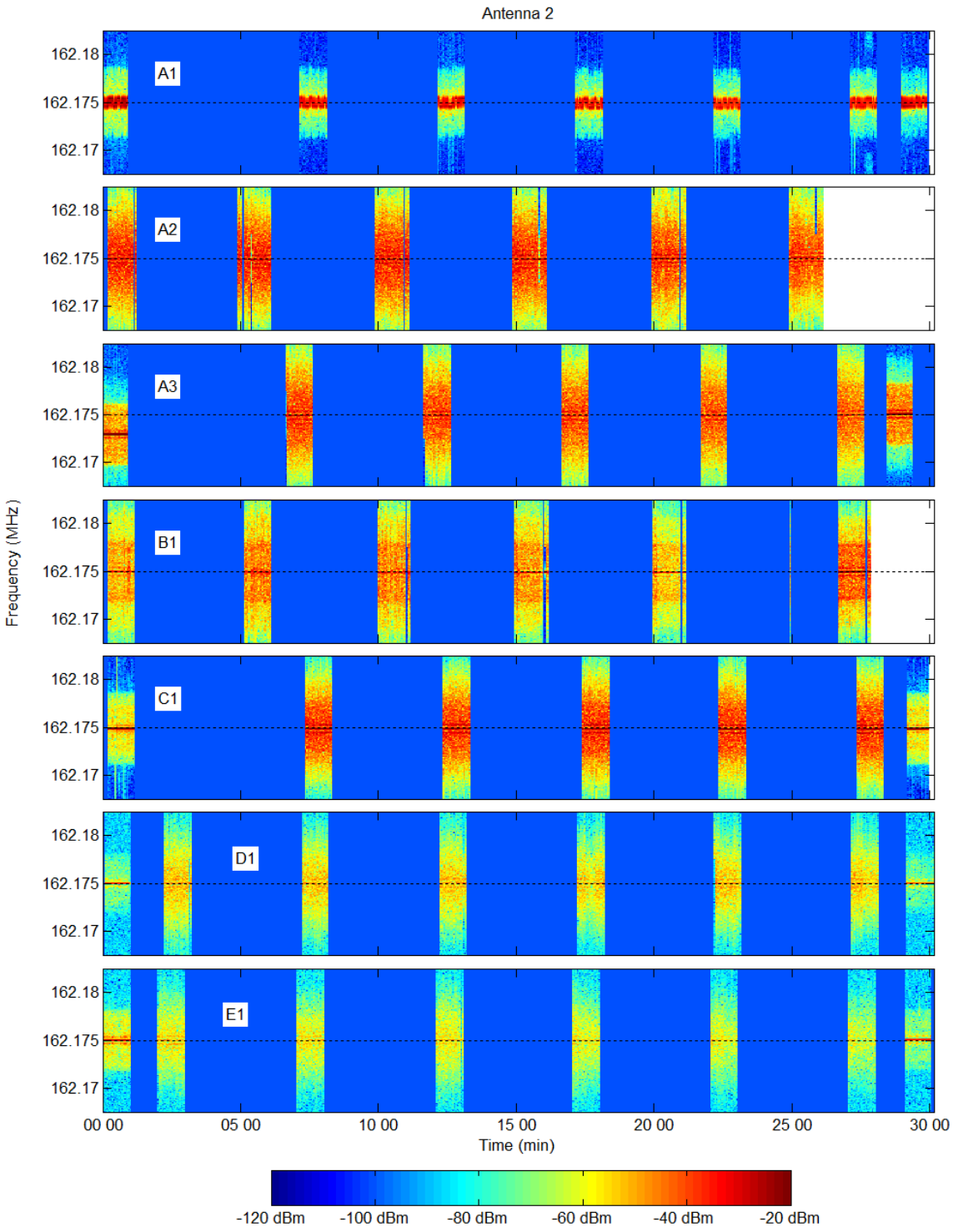

Figure 9. Results for Antenna 2 at 100 °C for 25 min. The letter labels correspond to the radio. The blue sections of the plots indicate the radio was not transmitting and the white sections indicate that the test was completed. The dotted center line represents the nominal frequency of 162.175 MHz.

This publication is available free of charge from http://dx.doi.org/10.6028/NIST.TN.1850

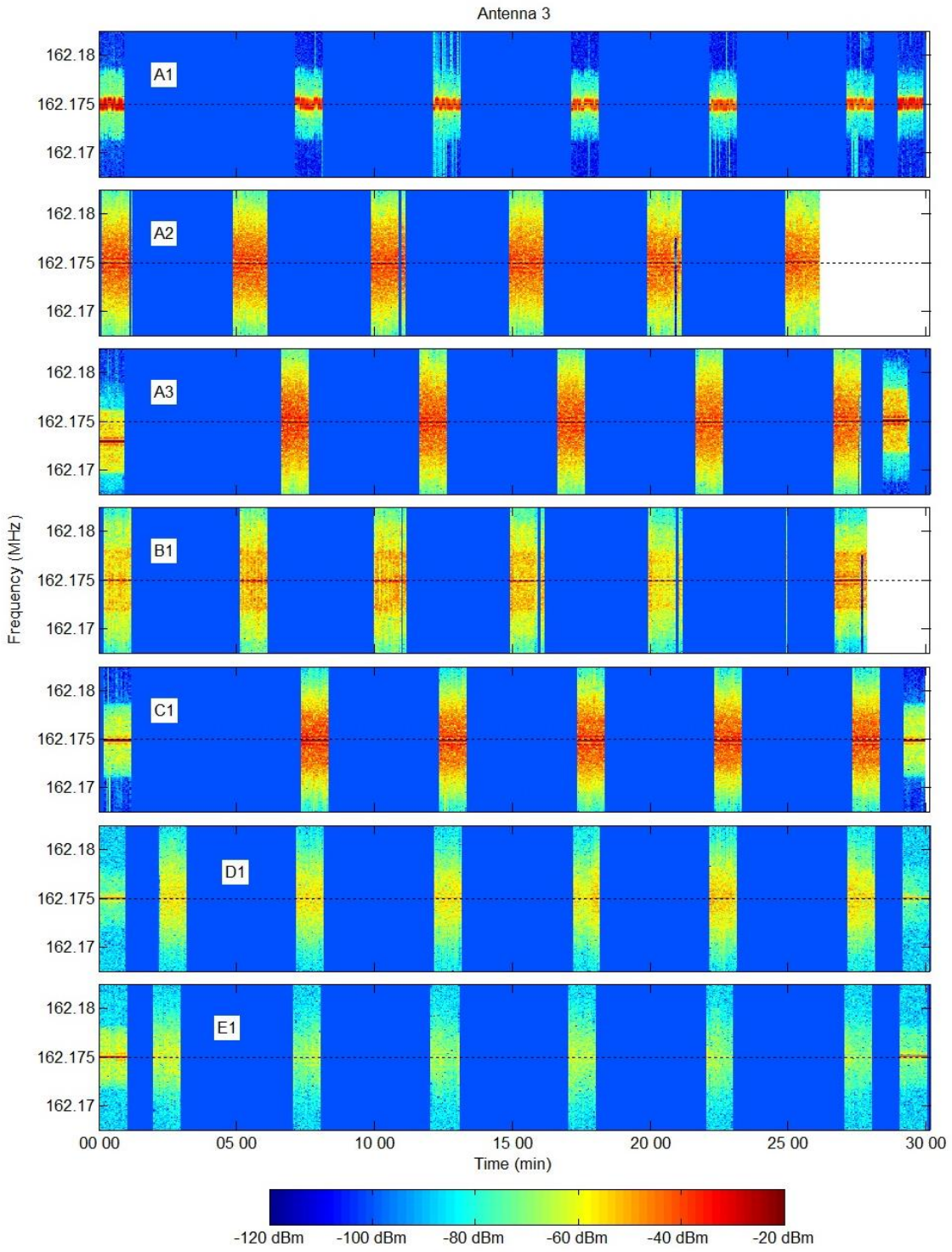

Figure 10. Results for Antenna 3 at 100 °C for 25 min. The letter labels correspond to the radio. The blue sections of the plots indicate the radio was not transmitting, and the white sections indicate that the test was completed. The dotted center line represents the nominal frequency of 162.175 MHz.

The carrier frequency behavior during the Thermal Class I tests at 100 °C for 15 min was determined from the aggregate data using the measurements collected from each of the three different antenna elements. Figure 11 shows the mean maximum-power frequency ± 1σ, as indicated by dash marks, and ± 2σ as indicated by triangles. The signal data are plotted as a function of time inside the flow loop. The designation BL on the plots indicates the baseline measurement of the radio frequency measured at ambient temperature while the radio was outside of the flow loop before the elevated temperature exposure test. The designation PT on the plots refers to the post-test measurements collected with the radio outside the flow loop immediately following the elevated temperature tests, before the radio had a chance to cool. Measurements plotted in Figure 11 correspond to the active regions shown in the spectrograms. For most of the measurements, the maximum-power frequency was very close to the mean maximum-power frequency. The only significant spread occurred in the measurement of radio B1 at 10 min inside the flow loop. It is not obvious why this variation occurred, but other measurements for radio B1 exhibited variations similar to the measurements for the other six radios.

Results for the baseline measurement for radio A3 are not shown because the radio was initially transmitting at a carrier frequency below 162.174 MHz. However, when the radio was placed in the flow loop, the radio transmitted with a carrier frequency of 162.175 MHz as programmed. The first measurement transmission is clearly evident in Figure 8 by the dark red line offset below the desired center frequency of 162.175 MHz. The cause of the initially incorrect carrier frequency was not identified. Post-test data for radio A2 and radio B1 are not shown because this data was not collected. These radios did operate immediately following the tests at 100 °C, but the data were not recorded.

Figure 12 shows the frequency deviation ± 1σ (indicated by dash marks) and ± 2σ (indicated by triangles) with respect to the carrier frequency of 162.175 MHz. As in Figure 11, baseline measurements before the tests are indicated by BL and post-test measurements are indicated by PT. For all cases, the deviation of the mean maximum-power frequency was less than 1 ppm. For the measurement of radio B1 at 10 min, 2σ = 11 ppm. For all the other measurements, 2σ was 6 ppm or less. Results at the Thermal Class I conditions of 100 °C for 25 min indicated that the carrier frequency of all the radios maintained good frequency stability during elevated temperature exposure.

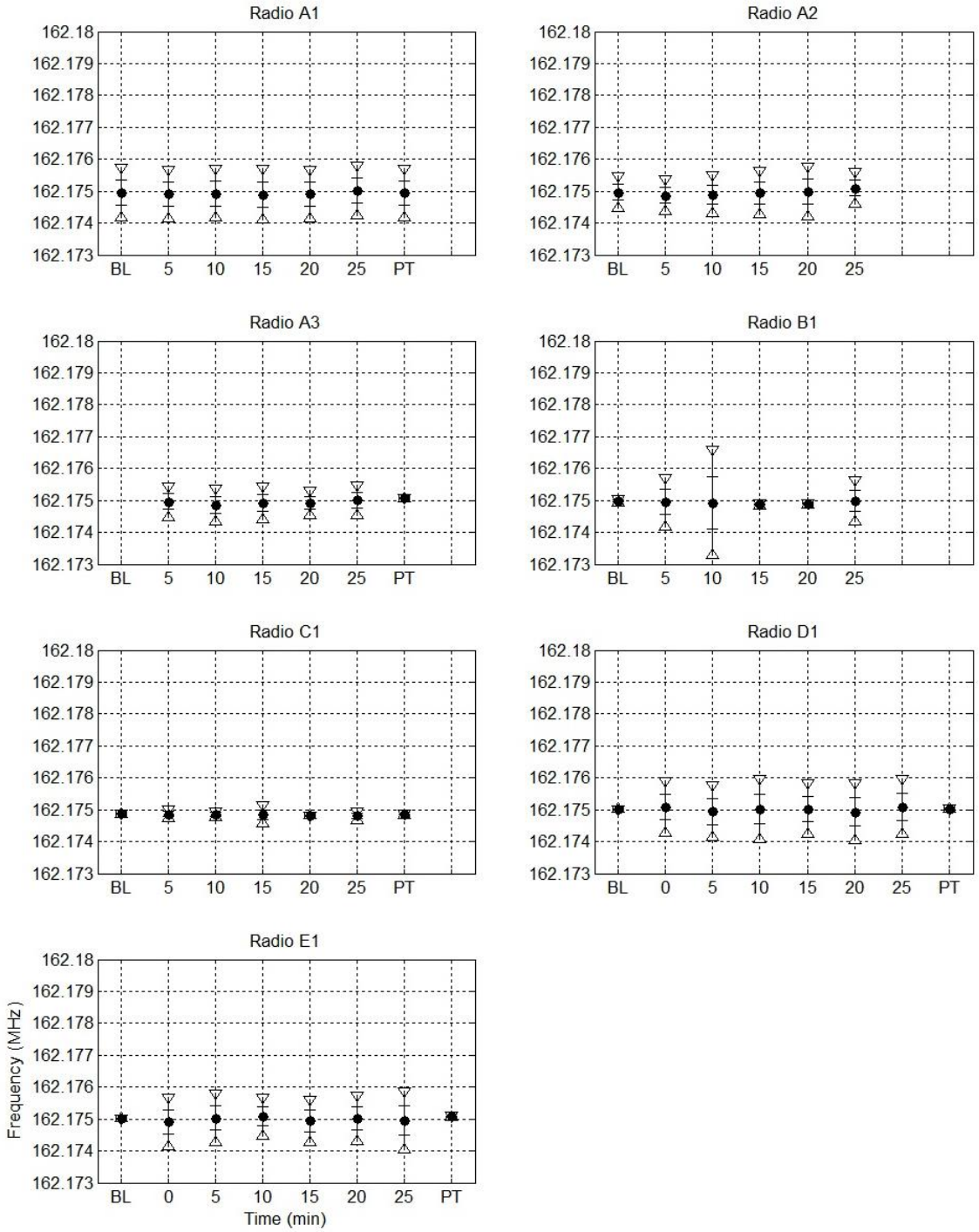

Figure 11. Mean maximum-power frequency ± 1σ (dash marks) and ± 2σ (triangles) for the radios exposed to 100° C. The data are aggregated using measurements from each of the three antenna elements. The number of data points per measurement was typically between 50 and 60 (approximately 17 to 20 per antenna element). BL represents baseline data collected outside the flow loop at ambient temperature before the test, and PT represents post-test data collected outside the flow loop, within 90 s following the elevated temperature test.

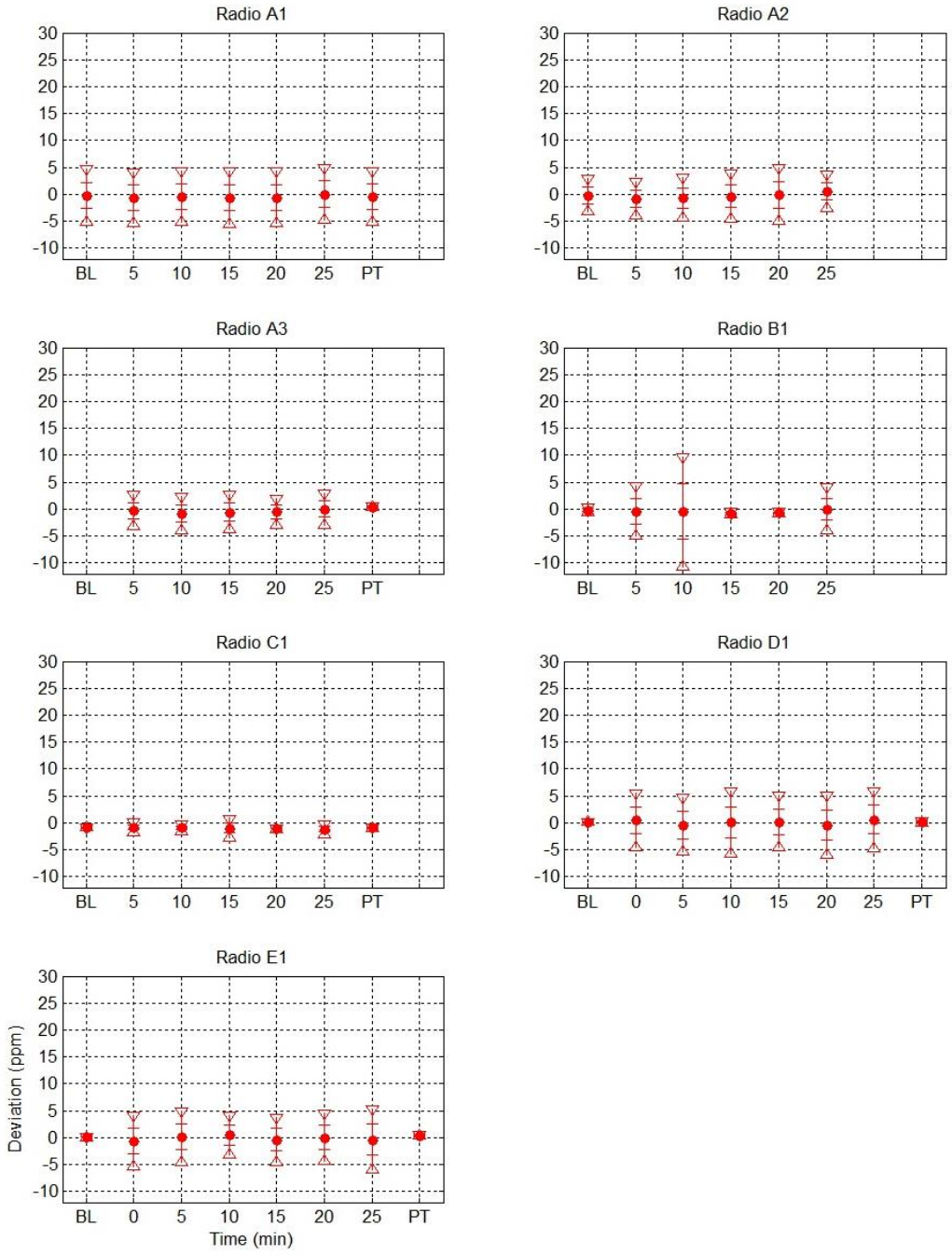

Figure 12. Mean maximum-power frequency deviation ± 1σ (dash marks) and ± 2σ (triangles) relative to 162.175 MHz for the 100° C tests. The data were aggregated from the measurements for each of three antenna elements, and the number of data points per measurement was typically between 50 and 60. BL represents baseline data collected outside the flow loop at ambient temperature before the test, and PT represents post-test data collected outside the flow loop, within 90 s following the elevated temperature test.

This publication is available free of charge from http://dx.doi.org/10.6028/NIST.TN.1850

Performance results for testing of fire fighter portable radios at Thermal Class I conditions of 100 °C for 25 min showed that the radios were able to maintain frequency stability of the maximum-power frequency. A summary of the results is shown in Table 2.

Table 2. Summary of Results for Radio Testing at Thermal Class I

Radio	Thermal Class I Exposure 100 °C for 25 min
A1	Radio signal maintained frequency stability.
A2	Radio signal maintained frequency stability.
A3	Radio signal maintained frequency stability.
B1	Radio signal maintained frequency stability.
C1	Radio signal maintained frequency stability.
D1	Radio signal maintained frequency stability.
E1	Radio signal maintained frequency stability.

160 °C Results

Experiments were conducted to measure the performance of portable radios at Thermal Class II conditions of 160 °C for 15 min. The results across the seven radios were not as uniform as the 100 °C tests. The spectrograms for antenna 1 are shown in Figure 13. Figure 14 and Figure 15 show results for antenna 2 and antenna 3, which are similar to those for antenna 1. For all radios, the first measurement is a baseline measurement that occurs with the radio outside of the flow loop, at ambient temperature. The dark red line of maximum-power indicates a carrier frequency of 162.175 MHz for all the radios.

In the case of radios A1, A2, A3, B1, and C1, the first signal measurement at 160 °C occurred three minutes after entering the flow loop. Radios D1 and E1 were tested immediately after entering the flow loop. The radio signals were then tested every three minutes for 15 min. As seen in the spectrograms, no radio signal was transmitted by radio A1, A3, B1, or C1 at 15 min. Additionally, radio A3 stopped transmitting 730 s (12 min + 10 s) after entering the flow loop. This is indicated by the very narrow band on the radio A3 spectrograms. After the tests at 160 °C, the radios were removed from the flow loop and a final RF signal was measured within 90 s of removal from the flow loop while the radios were still hot. When removed from the flow loop, both radio A1 and radio A3 were able to transmit, even though they had stopped transmitting when inside the flow loop. Radio B1 and radio C1 were not able to transmit, even after being removed from the flow loop.

Figure 16 shows the mean maximum-power frequency ± 1σ, indicated by dash marks, and ± 2σ indicated by triangles, for the tests at 160 °C. Data are plotted as a function of time inside the flow loop. As with the 100 °C tests, a baseline measurement of the radio frequency, designated as BL on the plots, was measured at ambient temperature while the radio was outside of the flow loop before the elevated temperature exposure. The designation PT on the plots refers to post-test measurements collected with the radio outside the flow loop immediately following the elevated temperature tests, before the radio had a chance to cool.

When the mean maximum-power of the frequency deviates from the initial carrier frequency, this corresponds to a drift in the carrier frequency. Figure 16 shows that all of the radios experienced some drift in the mean maximum-power frequency, and thus drift of the radio carrier frequency. Radios A1 and A3 stopped transmitting during the 15 min test at 160 °C, and then showed drifts in their carrier frequencies when tested after the elevated temperature exposure. Radios B1 and C1 slowed only a slight drift in frequency, but did not transmit at 15 min, and could not transmit post-test. Radios A2, D1, and E1 were able to transmit throughout the 15 min test; however, these three radios exhibited a significant frequency drift in the carrier frequency. It is interesting that the frequency drift continued after the radios were removed from the flow loop, as seen in the post-test measurements.

This publication is available free of charge from http://dx.doi.org/10.6028/NIST.TN.1850

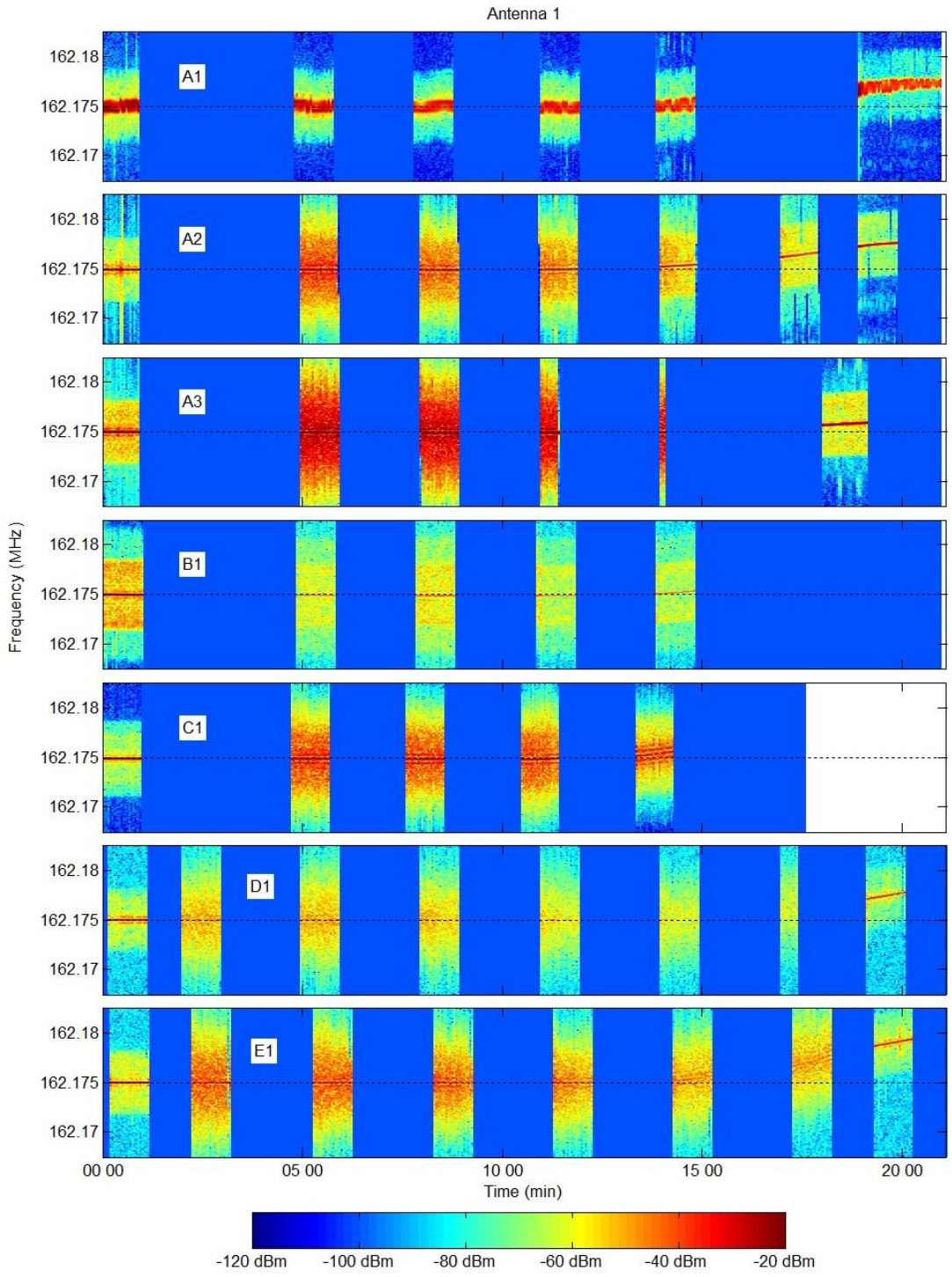

Figure 13. Power versus frequency and time measurement results for Antenna 1 at 160 °C for 15 min. A shift in frequency is indicated by the deep red section of the plots (i.e., the highest power) moving away from the dotted center line that represents the nominal frequency of 162.175 MHz.

This publication is available free of charge from http://dx.doi.org/10.6028/NIST.TN.1850

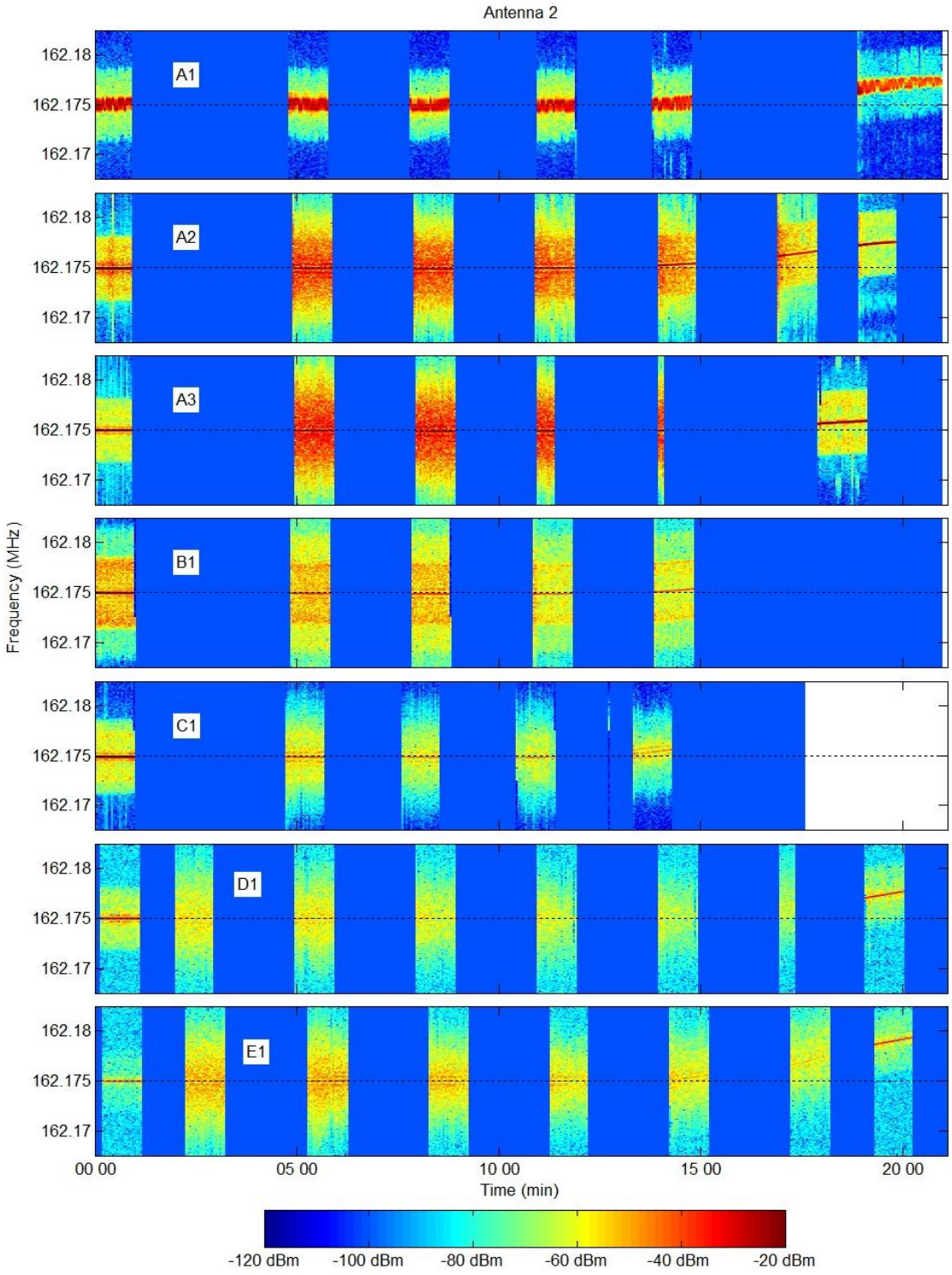

Figure 14. Results for Antenna 2 tested at 160 °C for 15 min. A shift in frequency is indicated by the deep red section of the plots moving away from the dotted center line that represents the nominal frequency of 162.175 MHz.

This publication is available free of charge from http://dx.doi.org/10.6028/NIST.TN.1850

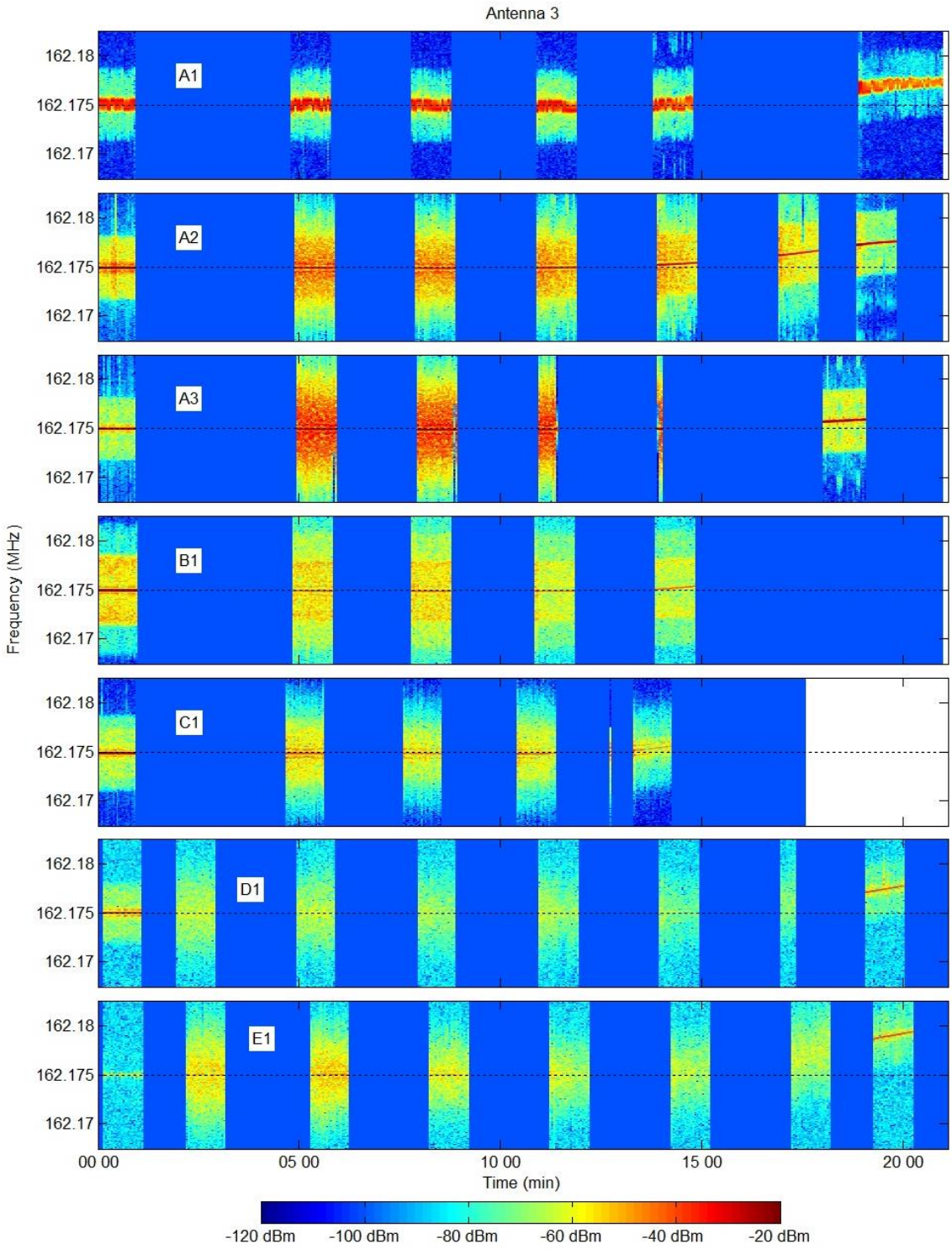

Figure 15. Results for Antenna 3 tested at 160 °C for 15 min. A shift in frequency is indicated by the deep red section of the plots moving away from the dotted center line that represents the nominal frequency of 162.175 MHz.

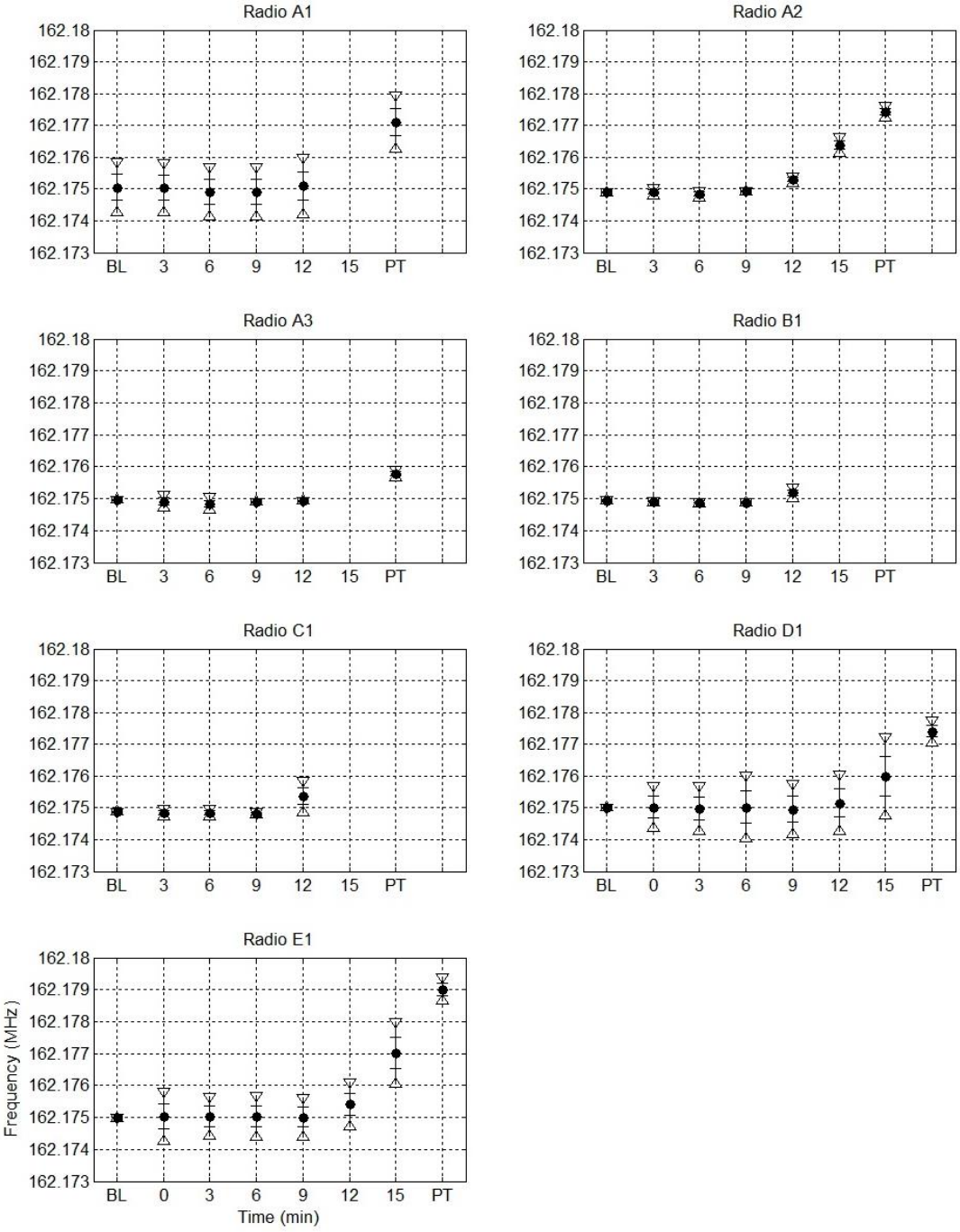

Figure 16. Mean maximum-power frequency ± 1σ (dash marks), and ± 2σ (triangles) for the 160 °C tests. The data are aggregated from the measurements for each of the three antenna elements, and the number of data points per measurement is typically between 50 and 60 (approximately 17-20 per antenna probe). BL represents baseline data collected outside the flow loop at ambient temperature before the test, and PT represents post-test data collected outside the flow loop, within 90 s following the elevated temperature test.

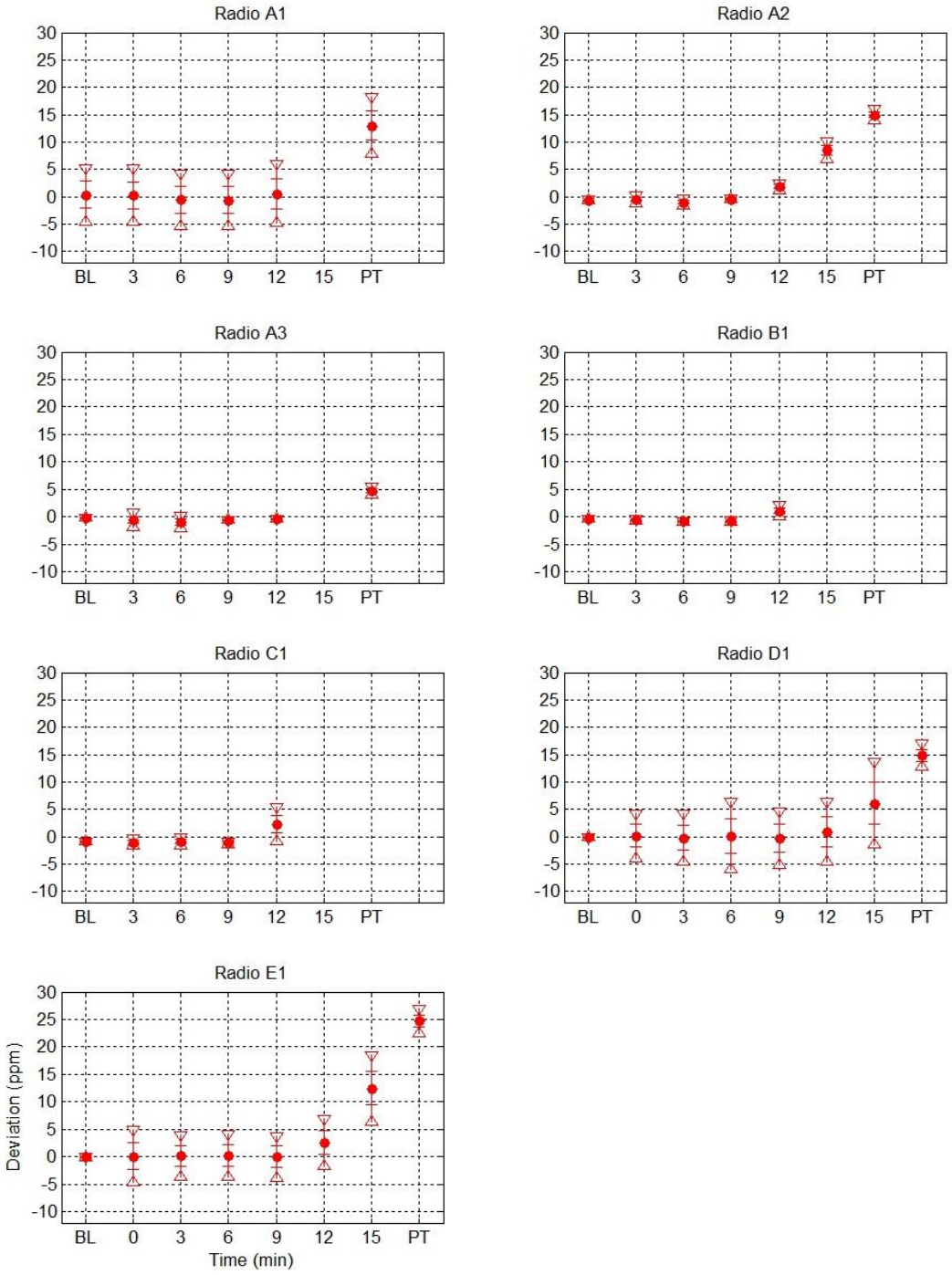

Figure 17. Mean maximum-power frequency deviation ± 1σ (dash marks), and ± 2σ (triangles) relative to 162.175 MHz for the 160 °C tests. The data were aggregated from the measurements for each of three antenna elements, and the number of data points per measurement was typically between 50 and 60. BL represents baseline data collected outside the flow loop at ambient temperature before the test, and PT represents post-test data collected outside the flow loop, within 90 s following the elevated temperature test.

The plots in figure 17 show the mean maximum-power frequency deviations relative to the nominal carrier frequency of 162.175 MHz. For radios A2, D1, and E1 the deviations of the mean maximum-power frequency exceeded 5 ppm for the transmissions at 15 min of 160 °C temperature exposure. For these three radios, the mean maximum-power frequency exceeded 10 ppm during the post-test measurement outside the flow loop, but before the radios had cooled. For radios A1, A3, B1, and C1, the deviations of the mean maximum-power frequency did not exceed 5 ppm, but these radios could not transmit after 15 min of exposure, and radios B1 and C1 could not transmit even after being removed from the flow loop. Radio A1 could transmit immediately after removal from the flow loop, but its mean maximum-power frequency was beyond 10 ppm.

Table 3. Summary of Results for Radio Testing at Thermal Class II

Radio	Thermal Class II Exposure 160 °C for 15 min
A1	No transmitting at 15 min. Signal drift of more than 5 ppm post-test.
A2	Signal drift of more than 5 ppm during test.
A3	Stopped transmitting at 12 min + 10 s (730 s).
B1	No transmitting at 15 min. Did not transmit post-test.
C1	No transmitting at 15 min. Did not transmit post-test.
D1	Signal drift of more than 5 ppm during test.
E1	Signal drift of more than 5 ppm during test.

The fire fighter portable radios tested at Thermal Class II conditions of 160 °C for 15 min exhibited problems maintaining performance. The results are summarized in Table 3. Four of the radios stopped transmitting during the 15 min test. The three radios that continued transmitting throughout the test experienced a frequency drift that was more than the 5 ppm specified by the TIA standard. Some of the radios tested were able to maintain frequency

stability through the first 12 min of Class II exposure. This may suggest that small changes may enable some radios to meet a Thermal Class II standard requirement.

Future Work

The experiments described here investigate the performance of portable radios exposed to Thermal Class I and Thermal Class II conditions. Work planned for the next phase of this project will expose the radios to Class III conditions of 260 °C for 5 min. Although the time duration is shorter, exposure to 260 °C represents an extreme temperature condition for operation of electronic equipment. Previous research conducted at temperatures above 160 °C suggests that the radios currently on the market will experience significant challenges maintaining an adequate level of performance at this temperature, even for short durations [1].

For the experiments discussed in this document, all testing of the radio transmission was performed in the VHF band at a frequency of 162.175 MHz. Because the oscillator circuity, other radio components, and housing materials are common to radios operating in other frequency bands such as UHF, similar results and frequency drift are also expected with those radios. Additional work is planned to investigate radio operation at elevated temperatures for frequencies in the UHF band.

Additional work planned in this area will also consider the impact of elevated temperatures on portable radio remote speaker microphone accessories. Preliminary testing of this equipment showed that it was also vulnerable to elevated temperatures [1]. Plans for further experiments include separate testing of the remote speaker microphone and the connecting cable assemblies to evaluate performance issues and identify potential weak links in the assemblies.

Conclusions

The impact of elevated temperatures on the performance of fire fighter portable radios was investigated to develop scientifically based standards for the radios. Radios were tested at elevated temperature conditions in the NIST thermal exposure flow loop. An RF sampling system measured the frequency signals from transmitting radios to measure their performance. Seven radios were tested at two different Thermal Class conditions, transmitting at a frequency of 162.175 MHz.

Radios were tested at Thermal Class I conditions of 100 °C for 25 min. All seven of the radios tested were able to transmit throughout the test durations. All of the radios maintained frequency stability of the maximum-power frequency throughout the tests.

Radios were tested at Thermal Class II conditions of 160 °C for 15 min. All of the radios tested experienced some type of performance problem during the testing. Four radios could not transmit throughout the 15 min of exposure to 160 °C temperatures. The remaining three radios were able to transmit throughout the 15 min test, but experienced signal drift of the mean maximum-power frequency, with a deviation from the carrier frequency that exceeded 5 ppm.

The results of these experiments indicate that exposure to Thermal Class II conditions (elevated temperature conditions of 160 °C for 15 min) can have adverse effects on radio performance, resulting in drift of the signal frequency and failure to transmit.

References

[1] Davis, W.D., Donnelly, M.K., and Selepak, M.J., "Testing of Portable Radios in a Fire Fighting Environment," National Institute of Standards and Technology, Gaithersburg, MD, NIST Technical Note 1477, August 2006.

[2] NIOSH Fire Fighter Fatality Investigation and Prevention Program, "A Career Lieutenant and Fire Fighter/Paramedic Die in a Hillside Residential House Fire – California," U.S. Department of Health and Human Services, Public Health Service, Centers for Disease Control and Prevention, National Institute for Occupational Safety and Health, DHHS (NIOSH) Publication No.# 2011-13.

[3] National Fire Protection Association, "NFPA 1221: Standard for Installation, Maintenance and Use of Emergency Services Communications Systems," 2013 Edition, National Fire Codes, Volume 12, Quincy, MA, 2014.

[4] Donnelly M. K., Davis W. D., Lawson, J. R., and Selepak, M. S., "Thermal Environment for Electronic Equipment used by First Responders," National Institute of Standards and Technology, Gaithersburg, MD, NIST Technical Note 1474, January 2006.

[5] Abeles, Fred J., "Protective Ensemble Performance Standards, Project Fires" Phase 1B Final Report, Volume 2, Grumman Aerospace Corporation, Bethpage, New York, May 1980.

[6] Abbott, N. J. and Schulman, S., "Protection from Fire: Nonflammable Fabrics and Coatings," Proceedings of 1976 International Symposium on Flammability and Fire Retardants. Ontario, Canada, May 6-7, 1976.

[7] Federal Emergency Management Agency/United States Fire Administration "Minimum Standards on Structural Fire Fighting Protective Clothing and Equipment: A Guide for Fire Service Education and Procurement," FA-137, United States Fire Administration, 16825 South Seton Avenue, Emmitsburg, MD 21727. December 1992.

[8] Foster, J. A., and Roberts, G.V., "Measurements of the Firefighting Environment – Summary Report," Central Fire Brigades Advisory Council Research Report number 61, 1994, Home Office Fire Research and Development Group, Fire Engineers Journal, United Kingdom, September 1995.

[9] Setra Model 264 Very Low Pressure Transducer Data Sheet Revision E. Setra Systems, Boxborough, MA., December 2002.

[10] Omega Engineering, Inc., The Omega Temperature Measurement Handbook and Encyclopedia, Vol. MMX 6th ed., Stamford, CT, Omega Engineering, 2007.

[11] Bandhauer, T.M., Garimella, S. and Fuller, T.F., "A Critical Review of Thermal Issues in Lithium-Ion BatteriesReviews - Critical Reviews in Electrochemistry and Solid-State Science and Technology," Journal of the Electrochemical Society, Vol. 158, 2011.

[12] Spotnitz, R. and Franklin, J., "Abuse of high-power, lithium-ion cells," Journal of Power Sources, Vol. 113, Issue 1, January 2003.

[13] Baginska, M., Blaiszik, B.J., Merriman, R.J., Sottos, N.R., Moore, J.S., and White, S.R., "Autonomic Shutdown of Lithium-Ion Batteries Using Thermoresponsive Mircrospheres," Advanced Energy Materials, 2012.

[14] Mandal, B.K., Padhi, A.K., Shi, Z., Chakraborty, S. and Filler, R., "Thermal runaway inhibitors for lithium battery electrolytes," Journal of Power Sources, Vol. 161, Issue 2, October 2006.

[15] "Land Mobile FM or PM Communications Equipment Measurement and Performance Standard," ANSI/TIA-603-D, 2010.

Acknowledgements

This work was sponsored the Department of Homeland Security (DHS) to advance the development of standards for electronic equipment used by emergency responders.

The authors would like to thank Keith Stakes of NIST for his assistance conducting some of the experiments and for creating the flow loop diagrams. The authors would also like to thank Roy McLane and Jay McElroy, both of NIST, for their assistance with the laboratory apparatus and instrumentation.

This publication is available free of charge from http://dx.doi.org/10.6028/NIST.TN.1850

Appendix A: Supplemental Figures

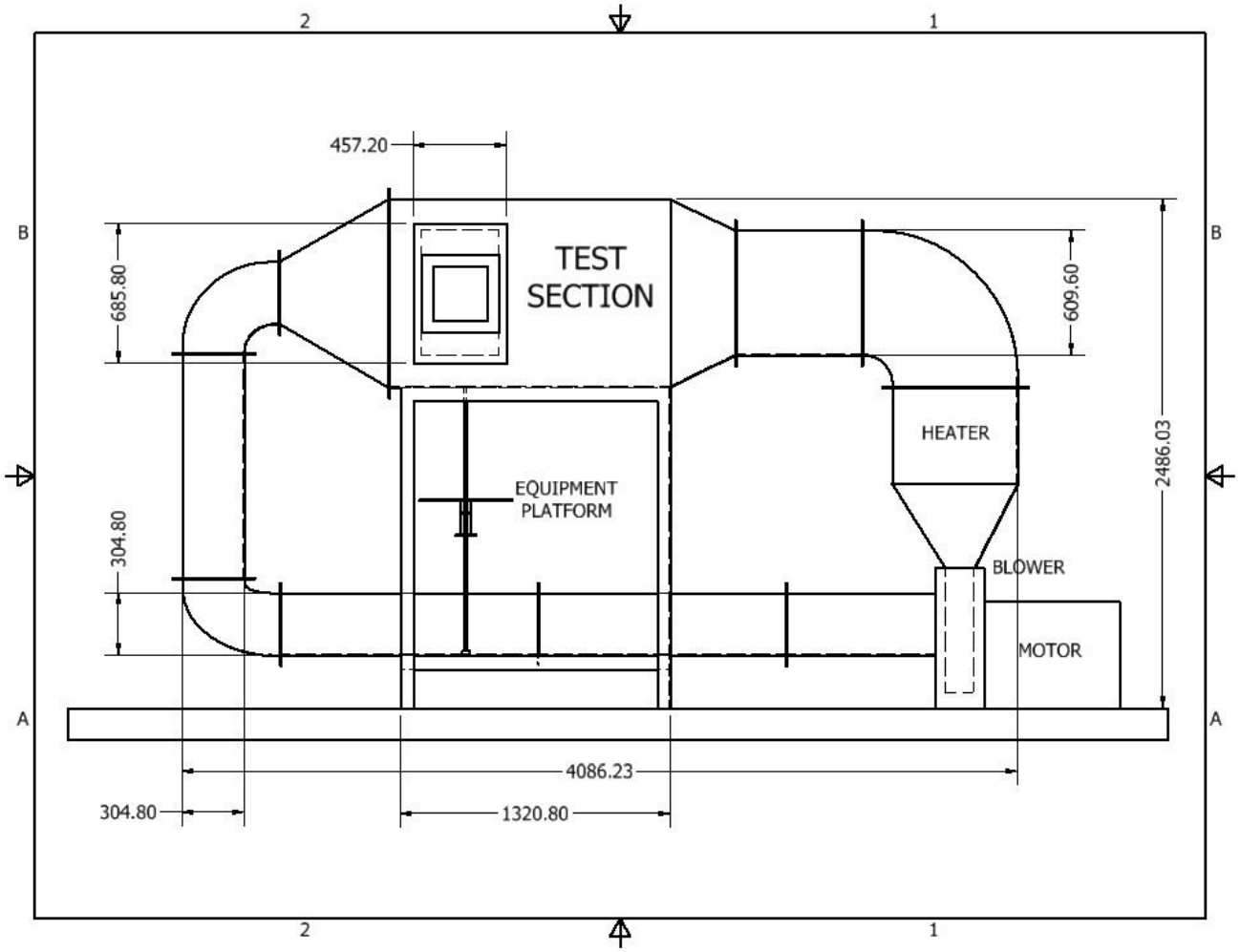

Figure A1. Diagram of the NIST Thermal Exposure Flow Loop. Dimensions are in mm.

This publication is available free of charge from http://dx.doi.org/10.6028/NIST.TN.1850

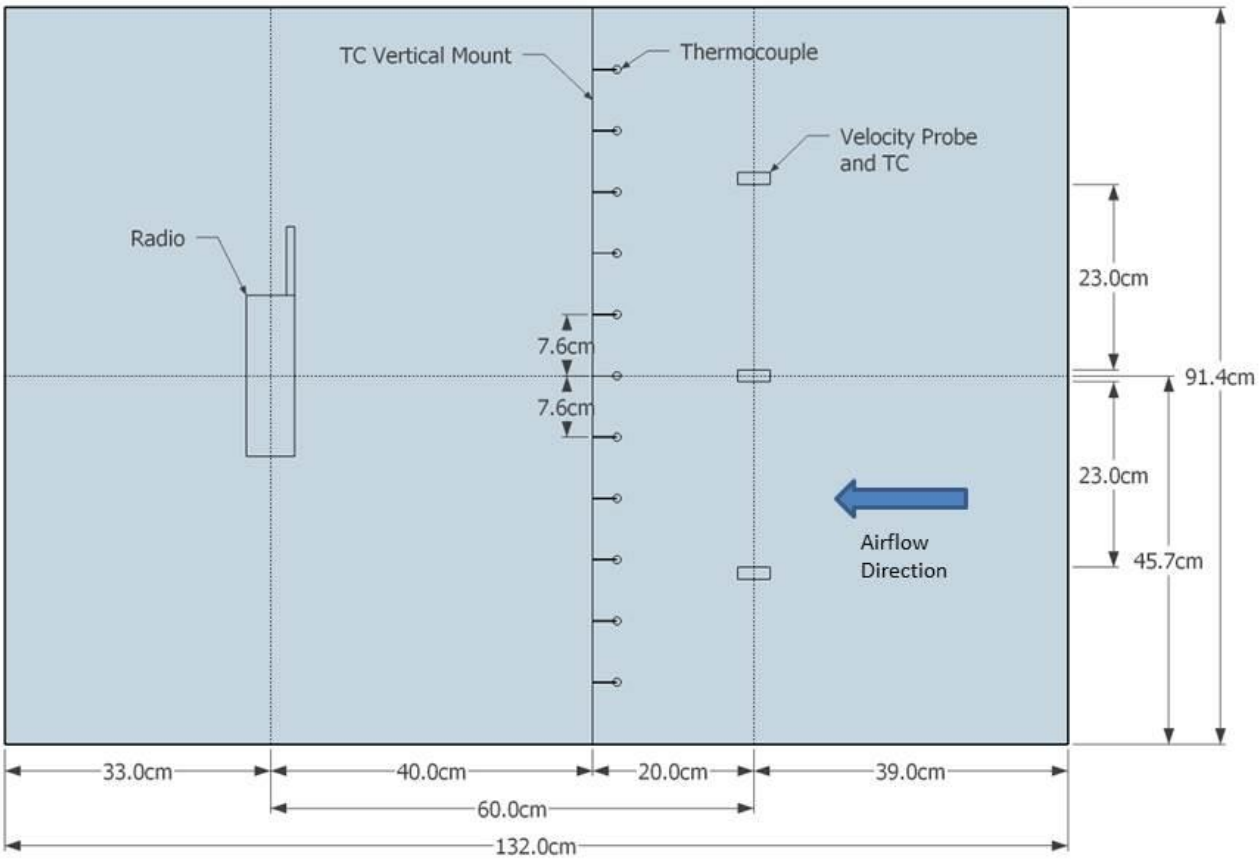

Figure A2. **Diagram showing a side view of the inside of the test section of the NIST Thermal Exposure Flow Loop. Dimensions are in cm.**

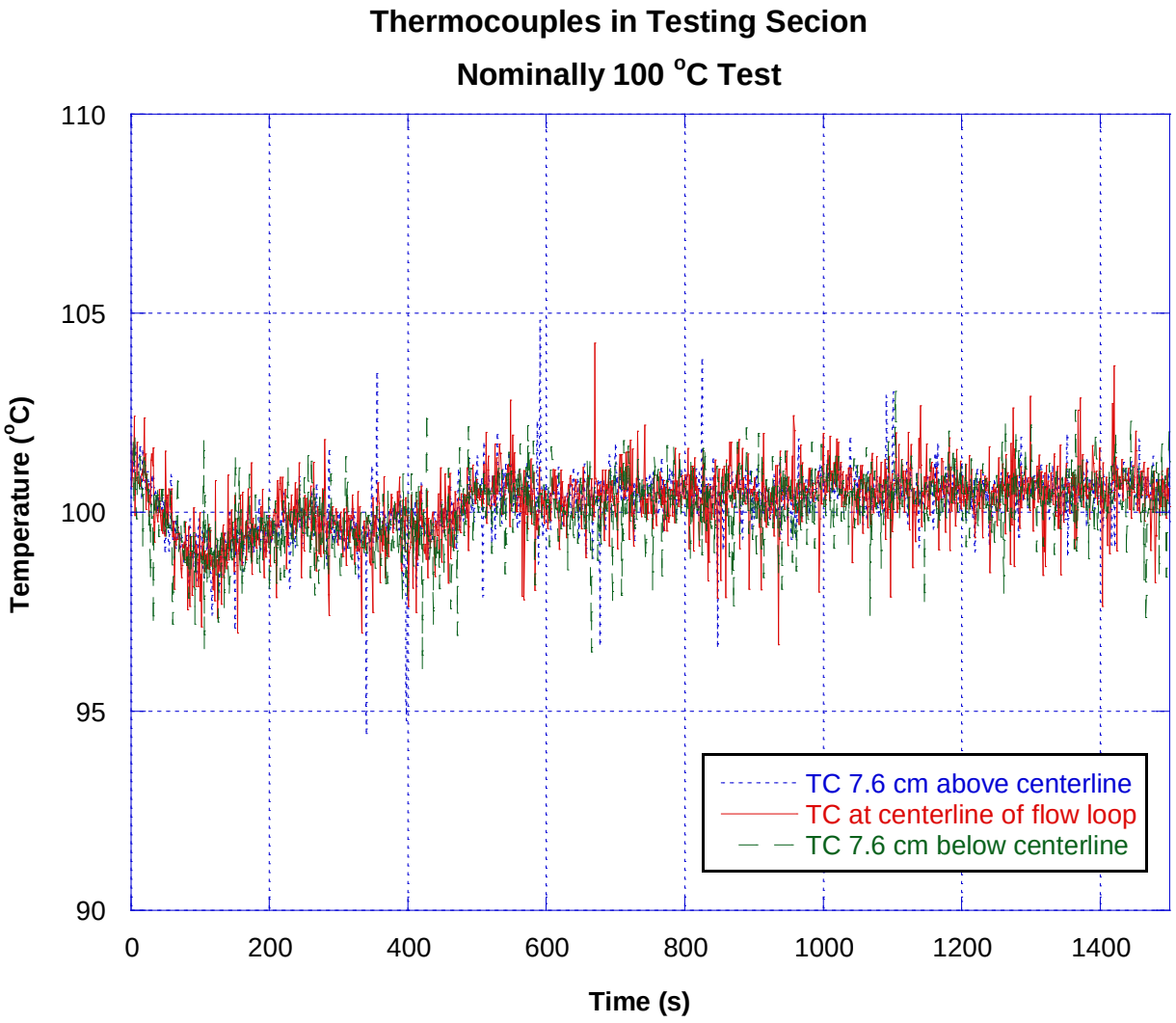

Figure A3. Example of temperature measurements inside the test section for a test at nominally 100 °C. The average temperature at the centerline is 100.2 °C, where 2σ = 1.7. The average temperature 7.6 cm above the centerline is 100.2 °C, where 2σ = 1.4, and the average temperature 7.6 cm below the centerline is 100.1 °C, with 2σ = 1.7.

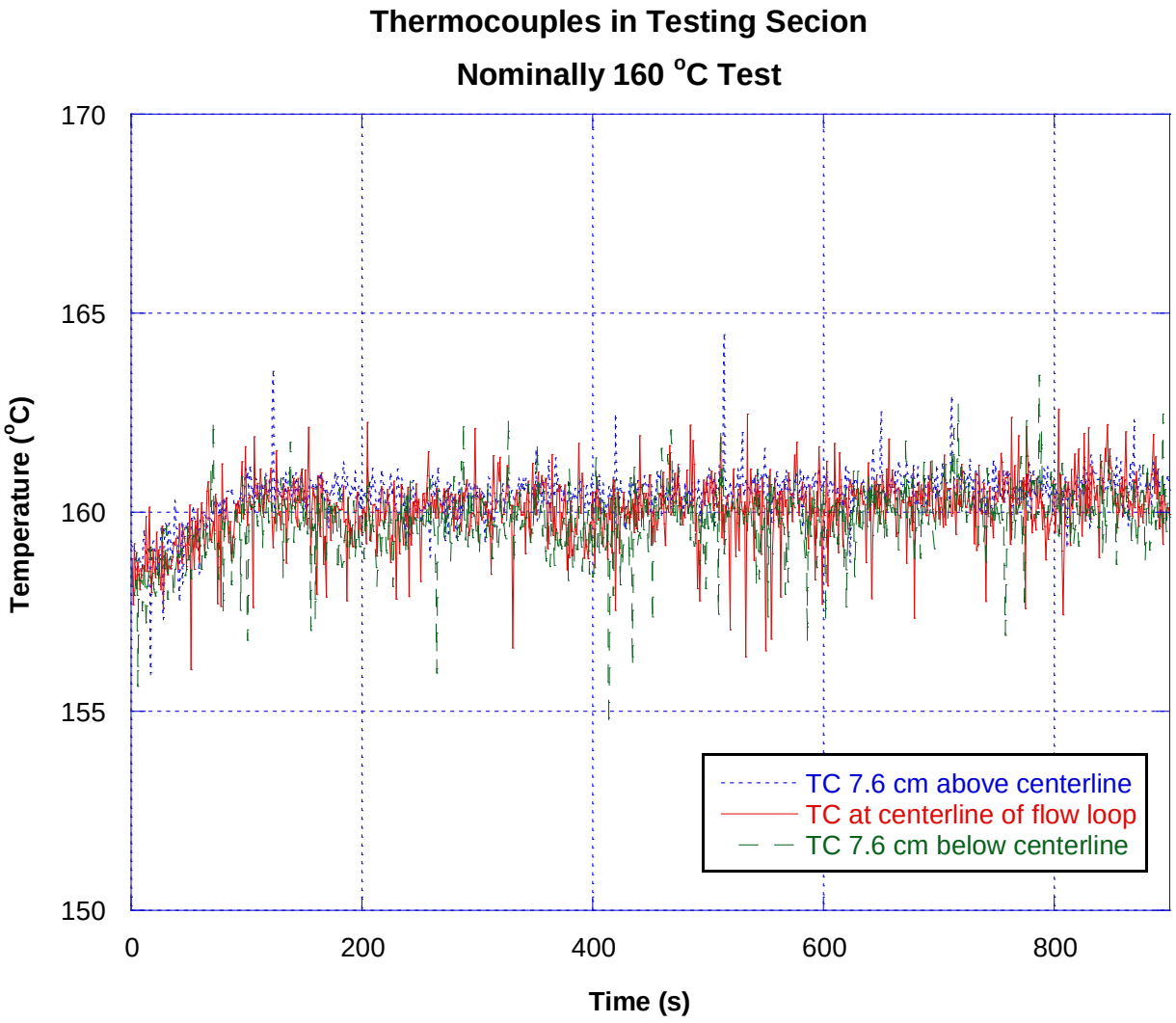

Figure A4. Example of temperature measurements inside the test section for a test at nominally 160 °C. The average temperature at the centerline is 160.1 °C, where 2σ = 1.7. The average temperature 7.6 cm above the centerline is 160.4 °C, where 2σ = 1.2, and the average temperature 7.6 cm below the centerline is 159.8 °C, with 2σ = 1.7.

This publication is available free of charge from http://dx.doi.org/10.6028/NIST.TN.1850

Appendix B: Overview of Power Levels on the Linear and Logarithm Scales

The measured power levels shown in this document are given on the decibel scale, which is a typical format in the communication industry. This logarithmic transformation to a decibel scale allows easier visualization and manipulation of the data than in the linear domain. For example, multiplication in the linear domain becomes addition in the logarithm domain. The magnitude of the measured signal powers are such that the resulting decibel values may be either positive or negative. Equations below show the conversion of a linear power quantity to a decibel scale. A key point in this transformation process is that the linear data are compared relative to a specified reference value, or in the case, one milliwatt (mW).

$$\text{power (dBm)} = 10 \times \log_{10}\left(\frac{\text{power}}{1\,\text{mW}}\right) \tag{B-1}$$

To convert back to a linear scale, the following equation is applied.

$$\text{power(mW)} = 10^{\frac{\text{power(dBm)}}{10}} \tag{B-2}$$

It is useful to look at three different cases when converting to the decibel scale. First, consider a measured signal of 5 watts (W), which is greater than 1 mW. Using (B-1), we calculate:

$$5\,\text{W} = 10 \times \log_{10}\left(\frac{5000\,\text{mW}}{1\,\text{mW}}\right) = 10 \times \log_{10}(5000) = 37\text{dBm}.$$

Next, consider 0.005 mW, which is less than 1 mW. Here (B-1) gives:

$$0.005\,\text{mW} = 10 \times \log_{10}\left(\frac{0.005\,\text{mW}}{1\,\text{mW}}\right) = 10 \times \log_{10}(0.005) = \text{-}23\,\text{dBm}.$$

Finally, consider 1 mW, which is equal to the 1 mW reference. Here (B-1) gives:

$$1\,\text{mW} = 10 \times \log_{10}\left(\frac{1\,\text{mW}}{1\,\text{mW}}\right) = 10 \times \log_{10}(1) = 0\,\text{dBm}.$$

Thus, even though the linear data are on a scale from 0 to $+\infty$, on the decibel scale the values can take on positive and negative values. The decibel representation allows ease in comparing a wide range in signal levels, e.g., a 5 W value to a 0.005 mW value is the same as comparing 37 dBm to -23 dBm. The difference on the decibel scale is 37 dBm – (- 23 dBm) = 60 dB, or a factor of 1,000,000. Ranges of this size and greater are common in communication systems.